Journal of Circular Economy (2026) 4:3, No. 33
https://doi.org/10.55845/pqdyx828

RESEARCH ARTICLE

Full-Scale Implementation of Sensor-Based Quality Monitoring for Construction and Demolition Waste Processing: A Case Study on Data Availability and Preliminary Implications for the Circular Economy

Lieve Göbbels[1*], Dietlind Ahrens[1], Karoline Raulf[1]

Received: 15 June 2026 / Accepted: 8 September 2026 / Published: 15 September 2026

Abstract

Current data gaps hinder an efficient sustainability transition of the construction sector. Simultaneously, at the intersection of data science and waste management, much research is being conducted to monitor quality factors of interest for material flows in recycling processes. In the past years, we developed and implemented a prototype sensor-based quality monitoring system to analyze the particle size distribution during processing of construction and demolition waste. In this work, we assess this prototype in terms of 1) contribution to data availability and thus closing the current data gap, and 2) its preliminary social, environmental and economic implications in the context of a circular economy. We find that our system can record data robustly, provide results timely and cover a significantly larger share of material (5.3–5.6 %) compared to the current state-of-the-art (<0.01 %). Additionally, preliminary implications regarding the social, environmental and economic aspects support the potential of our system to positively contribute to the transitioning towards a circular and sustainable construction sector. Nonetheless, further research is needed to solve persisting limitations regarding fine fractions and bulk monitoring and carrying out a holistic LCSA is considered valuable.

Keywords AI-based quality monitoring · quality management · construction and demolition waste · recycled building material · recycled concrete aggregates · particle size distribution · digitalization · environmental engineering · machine learning · deep learning · RGB-sensor · line scan recording

1. Introduction

In 2022, nearly 24 million tons of construction and demolition waste (CDW) were generated according to Germany's Federal Statistics Office (Eurostat, 2022). Additionally, in a 2022 study, the World Wide Fund for Nature estimated reduction potentials of up to 60 megatons of CO_2-equivalents and 66 megatons of resources (WWF Deutschland 2023). In the relatively new Substitute Building Materials Ordinance [Ersatzbaustoffverordnung] (EBV) (Bundesministerium für Umwelt, Klimaschutz, Naturschutz und nukleare Sicherheit, 2023) and several position papers, such as that of the German Council of Experts on Environmental Issues (Sachverständigenrat für Umweltfragen, 2026), the urgency of improving the environmental impacts the construction sector currently has is made clear. This is not just the case for Germany: recent estimates indicate CDW covering around 36 % of the overall global waste production (Alhawamdeh et al., 2024; Soto-Paz et al., 2023) of which a significant share is still landfilled (Kabirifar et al., 2020). Closing the loop, i.e. changing from linear to circular material flows, is one possible solution and an important step towards a more circular economy (CE) (Bocken et al., 2016; Kirchherr et al., 2018; Moustafa et al., 2025). There are different

[*] Corresponding author: lieve.goebbels@ants.rwth-aachen.de
[1] Institute for Anthropogenic Material Cycles – RWTH Aachen, Wüllnerstraße 2, 52062, Aachen, Germany.

understandings of the CE concept, but a popular definition is provided by Kirchherr et al.: “[it] describes an economic system that is based on business models which replace the ‘end-of-life’ concept with reducing, alternatively reusing, recycling and recovering materials in production/distribution and consumption processes [...]” (Kirchherr et al., 2017).

Improving circularity within the construction sector reasonably continues to be a popular focus in different research areas, such as designing sustainable buildings or structural elements (Kromoser et al., 2025; Mu et al., 2026; Tighnavard Balasbaneh & Ramadan, 2026), investigating selective demolition and its impact for reuse or recycling practices (Antunes et al., 2024; Bayram et al., 2025), or automation of material flow characterization for more transparent data on the quality of recyclable material in the post-use phase (Kroell et al., 2025). Since data availability is an important aspect of the CE (Bellini & Bang, 2022; Kirchherr et al., 2018), the latter topic is relevant in the transition towards a circular and sustainable construction sector, where large data gaps exist to this day (Osei-Tutu et al., 2023).

To fill these gaps, at the intersection of data science and waste management, much research is being conducted on how the combination of AI and physical sensors can be used to characterize features of interest from the construction and demolition waste (CDW) material stream. For instance, Li et al. describe a promising multi-sensor setup for material classification on laboratory scale (Li et al., 2022). With a similar focus on sensor-based sorting, Kronenwett et al. show the potential of using AI-based procedures by analyzing the classification and identification performance on a custom synthetic data set with different particle occlusion rates (Kronenwett et al., 2024). In a previous study, we investigated the performance of different deep learning architectures for predicting the volume-based particle size distribution (PSD) from single-particle grayscale volume (image) data acquired with a 3D-laser triangulation (3D-LT) sensor (Kroell et al., 2025). However, to the authors’ knowledge, studies describing the performance of sensor-based quality monitoring (SBQM) solutions in full-scale CDW processing plants or on data recorded in such plants are currently lacking. We consider this a crucial aspect for efficient development of such solutions for quality monitoring of CDW, given the high complexity of this material stream and the rough environment of CDW processing (Müller & Martins, 2022) which are generally severely simplified during primary, laboratory-scale developments, thereby limiting easy transfer of developments onto higher-scale applications.

As a building block in this research domain and to fill the current lack of research that describes upscaling AI- and sensor-based material flow characterization to function in full-scale plants, we conducted such investigations in the KIMBA project. Here, for the first time, a sensor- and AI-based quality monitoring system was implemented in a full-scale plant, over a conveyor belt, to investigate the feasibility of automating monitoring of the PSD — being one of the main quality indicators for recycled aggregates (RA) — for the output of mobile comminution plants. As such, in this work, the procedure and central results of the full-scale implementation of the quality monitoring system are described in the form of a case study, in particular regarding data availability. What is more, we describe the implications regarding acquired data for circular economy (CE) developments compared to the current status quo, i.e. manual sampling and at-line laboratory sieve analysis. So, the contribution of this work is two-fold. On the one hand, we aim to show the potential of the developed quality monitoring system. On the other hand, we also want to share our experiences and lessons learned during upscaling our SBQM system and finalizing its prototype development for a first full-scale plant implementation. This may boost efficient development of similar technical solutions that increase high-level recycling rates, thereby supporting transitioning towards a circular and sustainable construction sector.

1.1. Related Work

With AI and the required capacities becoming more widespread and accessible, deep learning technologies are increasingly being examined as potential solutions for the analysis of (optical) quality factors (Kroell et al., 2022; Lubongo et al., 2024). For instance, the work by Chang et al. covers multiple quality factors, including the volume-based PSD (Chang et al., 2025). This work shows promising results of using 3D-LT scanning in a containerized setup away from the End-of-Life (EoL) crushing facility to estimate the PSD under controlled, pilot-scale conditions. Assuming distributional uniformity and consistency within the assessed material flow, point clouds were fitted into ellipsoidal models, which morphological information were then aggregated into PSDs. As the authors indicate in the limitations, implementation on a full-scale plant requires further developments, especially with respect to existing operational constraints, the significant computational demand, scalability and economic viability.

In terms of computational demand and corresponding environmental impacts, Falk et al. (Falk et al., 2026) have conducted a detailed multi-criteria cradle-to-grave analysis on one of the most common heavy-weight GPUs, namely a Nvidia A100 SXM 40 GB GPU, in the context of frontier Large Language Models (LLMs). In this study, they found among other things that training of two frontier models from 2022–2023 is equivalent to the planetary boundaries budget (European Commission. Joint Research Centre., 2018) of 53 to 11,500 inhabitants, depending on the model and location of training. Because of the high energy demand of such models, similarly high impacts were found for the category (fossil fuel) resource use, with equivalence of planetary boundaries budget of 186 to 3,900 inhabitants. Even though the types of GPUs and AI models generally used for deep learning developments in the context of CDW monitoring are less heavy-weight or large compared to those used by Falk et al., taking such additional impacts into consideration is nonetheless important to determine whether the envisioned solution may truly be beneficial for the development of a circular and sustainable construction sector.

On a lower technology readiness level (TRL) compared to the aforementioned work (Chang et al., 2025), we acquired promising results regarding the use of 3D-LT scanning and convolutional neural networks (CNNs) in a previous study (Kroell et al., 2025). Here, we transformed single-particle point cloud-based data to grayscale images embedding volumetric information and used these images to train several deep learning models. Validating this approach on unseen data resulted in PSD errors of merely 1 vol% for the best-performing models. However, implementing this technology on a full scale, especially in the context of mobile comminution, has not yet been successful due to the rough environment and severe economic constraints concerning CDW processing (A. Di Maria et al., 2018; Kranert, 2024; Varli et al., 2026).

In an ongoing Austrian project focused on the development of an autonomous mobile crushing unit, an RGB-D approach is taken, where multiple RGB sensors capture the material flow from different angles to predict the PSD at the feed hopper (input) and on the discharge conveyor. This method is to be validated on a real mobile comminution unit, but results of the laboratory digital twin analysis indicate the potential of using RGB instead of 3D-LT (Skosareva et al. 2026). That RGB may sufficiently capture features underlying the PSD is also indicated by one of the first works in this research area: Di Maria et al. describe how look-up catalogs can be used (F. Di Maria et al., 2016). Nonetheless, the look-up approach is inherently at- or off-line, rendering it unsuitable for real-time SBQM.

Next to developments on the technical level, research is being conducted on the environmental, social and economic impacts that major changes in construction-related processing and recycling chains may have, including the impacts of recycled material quality (Backes & Traverso, 2021; Bayram et al., 2025; Bayram & Greiff, 2023). The three sustainability dimensions – environmental, social and economic – play an important role in the context of CE as its main goal is to accomplish sustainable development, which encompasses the simultaneous achievement of environmental quality, economic prosperity and social equity (Kirchherr et al., 2017). Consequently, Padilla-Rivera et al. investigate which social indicators are most important when assessing CE strategies (Padilla-Rivera et al., 2021). They find that consumer health and safety is the most important indicator, which is a highly relevant factor in the construction sector. Additionally, Ruismäki et al. and Çetin et al. (Çetin et al., 2023; Ruismäki et al., 2025) investigate required information for digital product passports (DPPs) for construction products and material passports in the context of circularity in the construction sector. An aspect that is covered in both passports is the detailed information on material properties, which indicates downstream relevance of monitored aggregate production processes for material reuse. There are many factors related to the economic dimension, as indicated by Backes and Traverso (Backes & Traverso, 2021). In the context of CDW recycling plants and technical innovation, the willingness to pay (WTP) for recycled (concrete) aggregates (R(C)A) is one of the most important ones (Varli et al., 2026). In the discussion paper by Sterk (Sterk, 2023), an elaborate investigation on the WTP for RA in Germany is presented, where for instance clear labeling of the material leads to significant increase in the price a customer is willing to pay. This suggests that increased transparency at the start of the recycling process has implications for the economic as well as the social aspects, next to the environmental benefits optimal recycling and use of RA may bring.

1.2. Aims and Research Questions

Given the potential of RGB and encountered limitations of 3D-LT technology, as indicated in the related work that is part of the project on which this case study is based, we developed an RGB line scan-based quality monitoring system targeting the weight-based PSD on the discharge conveyor of a mobile comminution unit. The development process of the customized deep learning architectures for the different parts of the data processing pipeline — i.e. segmentation as pre-processing step and the weight-based PSD prediction — are detailed in separate publications (Zhou et al., 2025) and (Göbbels et al., 2026), respectively. Instead, in this case study, the aim is to analyze the overarching technical aspects of the system as well as to provide a first, albeit non-exhaustive, valuation of the social, environmental and economic implications. Correspondingly, two research questions are central to this work:

- RQ1: To what extent does the developed quality monitoring system contribute to data availability in the context of CDW processing for a circular and sustainable construction sector?
- RQ2: How may the developed quality monitoring system affect the social, environmental and economic aspects at a CDW processing plant?

To do so, we first focus on assessing the recording constancy, the data coverage at the end of the data processing pipeline, and the time it takes to process newly incoming images and output the predicted PSD. In the current work, it is impossible to exhaustively assess each individual aspect, however we deem it important to provide (post-hoc) insights into the impact our technical solution may have on the sector, when it comes to CE developments in the short- and medium-term. For the social aspect, we focus on two indicators (i.e. employee training and product labeling) that are important according to the literature and are feasible to determine post-hoc. For the environmental implications, we conducted a simplified, comparative, cradle-to-gate life cycle assessment (LCA) to analyze the avoided impacts associated with the application of recycled concrete aggregate in road versus building constructions as opposed to primary gravel. Lastly, for the economic aspects we combine findings from our technical, social and environmental analyses with available cost and price ranges. Where possible, we aim to use data available from the project (Varli et al., 2026), but approximations are inevitable due the post-hoc nature of the CE-analysis. By considering all core aspects of developing a technological innovation for a CDW recycling plant in the context of the CE, we hope to boost efficient development of similar technical solutions that optimize the recycling flow and support transitioning towards a circular and sustainable construction sector.

2. Materials and Methods

2.1. Sampling Campaigns and Sieve Analysis

During the project, several experiment campaigns have been conducted on a real CDW processing plant in Germany. For each campaign, the same mobile impact crusher was used, where the focus was on the output of the fine grain conveyor — above which the RGB sensor system was mounted. For the main sampling campaigns, we used 2,000 Mg of raw input material, containing mainly concrete, bricks and tiles. In Figure 1, the raw input material as well as the classified material are shown. Except for systematic adjustment of a subset of machine parameters and more frequent and methodical sampling, processing of the raw CDW input material remained similar to regular operation.

(**a**) (**b**)

Figure 1. (a) Raw, non-comminuted input material (b) Material after comminution and sieve classification

Each sample was taken using the same procedure: a small wheel loader equipped with a sampling hopper was positioned directly opposite of the material stream and 1) moved forward, 2) halted, and 3) moved backward in one flowing motion with a duration of 1 to 3 seconds, depending on the throughput. So, the aim was to acquire samples with approximately similar sizes. While taking a sample, a timestamp of the start of the sampling acquisition (i.e. when the first particles entered the hopper) was collected and documented, along with the duration of the sampling. After each sampling with the wheel loader, the sample was deposited in 90–liter containers, after which the material was manually subdivided into buckets for easier sample handling — not to homogenize the sample, as this is irrelevant for the goal at hand. Using this procedure, two sets of experiments were conducted: A (experiments conducted in February 2025), and B (experiments conducted in April 2025). Experiments within each set took place on the same day to minimize confounding.

Additionally, a demonstration experiment (C) was conducted in July of the same year. In two rounds, one with low throughput and the other with medium throughput ceteris paribus, the generic functionality of the system prototype was investigated. During this experiment, the sampling approach was adjusted slightly. More specifically, the sampling duration was extended to around 10 seconds to increase the span captured by the RGB sensor. RGB image data were acquired using custom python-based recording software. With this software, images were labeled with a nanosecond-specific GPS timestamp and saved for further analysis. This also allows additional developments on the pipeline (see Figure 2 for an outline) and deep learning models after the experiments have taken place. In Table 1, an overview of the main experiment campaigns is provided.

In this case study, the target output fraction is unbound concrete mixture aggregate with size indication 0/45. As such, the sampled material was processed in line with DIN EN 13285 (Deutsches Institut für Normung e.V., 2018). This includes size classification and determination of the percent by weight (wt%) of each class using laboratory sieve analysis. Following DIN EN 13285 and the procedure conducted by the laboratory personnel on the plant, the following screen undersizes were used: 0.063 mm, 0.5 mm, 1 mm, 2 mm, 4 mm, 5.6 mm, 8 mm, 11.2 mm, 16 mm, 22.4 mm, 31.5 mm, and 63 mm. The sampling campaigns and subsequent sieve analysis were conducted to acquire information on the PSD, which can be linked to the images that were simultaneously being recorded.

Table 1. Overview of the experiment campaigns

ID	Month, year	# Experiments	Description
A	February, 2025	7	Data and sample collection
B	April, 2025	7	Data and sample collection
C	July, 2025	1	Assessment of generic system functionality, collection of two samples

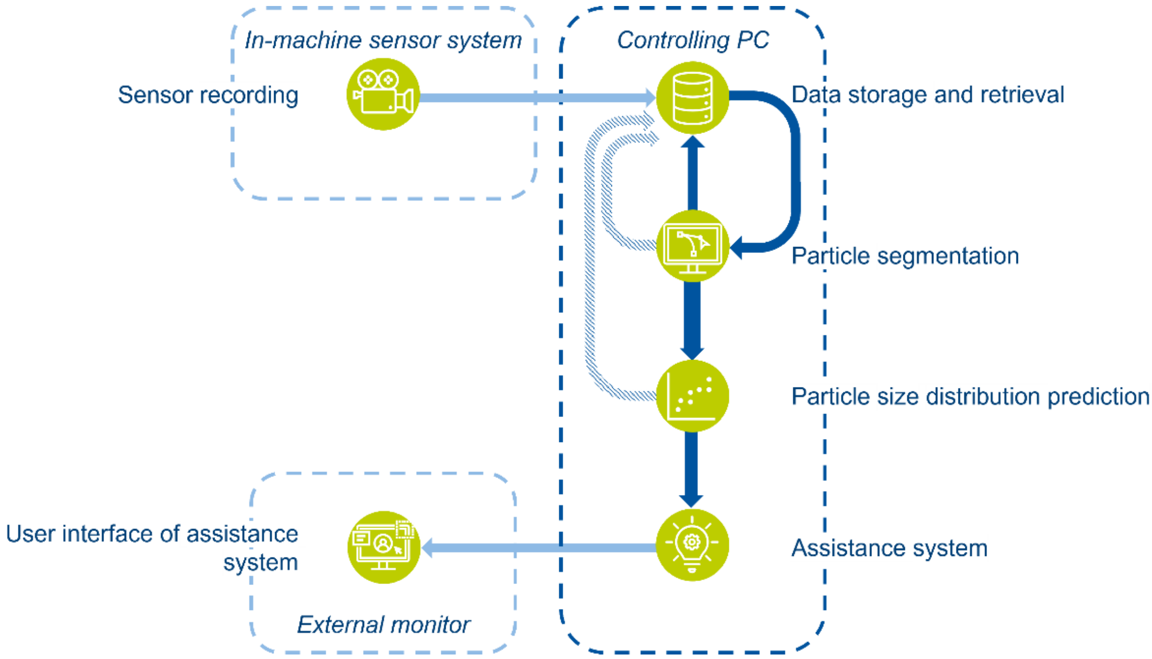

Figure 2. Graphical representation of the used quality monitoring system

2.2. Methods

2.2.1. Recording Constancy As part of the investigations on data availability, it is essential to analyze the recording frequency and to which extent this frequency fluctuates. To do so, as previously indicated, we documented the timestamp of each recorded image. This allows further analysis of the recording time series, in particular by means of time series analysis and visual interpretation. Additionally, during the campaigns the start and end time of each experiment was documented, which allows more targeted analysis.

For each experiment, the number of images recorded per minute was determined, after which the time series was assessed in terms of autocorrelation and stationarity, by autocorrelation function analysis and performing the augmented Dickey-Fuller (ADF)-test, respectively. The former allows identifying the presence of correlation of the time series with itself, where autocorrelation bars exceeding the significance bounds indicate significant autocorrelation at that particular lag (i.e. delay between observed data point and preceding values), a gradual decline indicates long-term dependency, and regular spikes indicate seasonality (Blackledge, 2005). The ADF-test statistically assesses the likely presence of a unit root, implying non-stationarity. That is, a unit root indicates stochastic trends that drive a time series away from its mean value. In this test, the null-hypothesis of non-stationarity is rejected when the test statistic is lower than the critical value at a specified significance level and the p-value is less than the specified significance level (Guo, 2023).

To determine whether the range of fluctuations is similar for the different sets of experiments, Levene's test for equality of variances is used. After identifying irregularities for each individual experiment in the previous steps, we can further clean this data and remove major irregularities, such as interruptions (e.g. due to power failure). Having both a minimally cleaned set as well as the original, we can compare the experiments 1) from the same day, 2) from different days, which is directly a different time of the year, and 3) the cleaned and original data. Since the p-value stemming from the Levene's test may be misleading for small samples, we also acquired the random test p-values on the basis of perturbation tests (Ludbrook & Dudley, 1998). If the p-value is low (and the Levene statistic is high), the null-hypothesis of equality is rejected. So, this test is merely strong proof of non-equality, but thereby gives a weak indication if two or more sets may be equal.

2.2.2. Data Coverage Since the prediction of the PSD is based on the visible top-layer of the material stream only, it makes sense to investigate to what extent the prediction covers the material stream compared to the whole and, not less important, compared to the current manual sampling. To this extent, we use the two best models from our previous work (Göbbels et al., 2026), as well as an additional model based on this architecture but equipped with a different – lighter, and thus faster – regression head to infer the particle weight and class from the particles segmented by ParticleSAM in the preceding pipeline module. We apply this procedure to set C in particular, since this set of experiments contains longer sampling durations and therefore more images, which minimizes the discrepancy between true sample and recorded material. Using the average of the weight prediction results of these models, we calculate the micro-average to get an idea of the overall, class-independent coverage. This average is calculated by taking the average of the sum of weight predictions and dividing this by the true weight of the sample. Additionally, we use the (%Δ wt per class) results on the unseen test set, also from our previous work (Göbbels et al., 2026), as error or sensitivity bounds and compare these results with the results from our manual sampling and sieve analysis to approximate the likely coverage possible by the models. All three models achieved overall classification accuracies of around 82 % and MAEs of less than 7 grams when processing the data set from our previous study. It must be noted that this performance result is only indicative and does not present model validation in an industrial implementation setting, which is considered out of scope in the current study.

2.2.3. Processing time For an analysis of the processing time of the different core components within the pipeline (see Figure 2), i.e. the image segmentation and the PSD prediction, we have transformed the pipeline in such a way that a live process can be simulated. This allows post-hoc analysis of the models' inference time, but also the influence of different levels of verbosity. For this, all 296 images with a corresponding sample analysis result are used in this simulation. These images stem from all experiment sets, and thus images recorded on three different occasions. The simulation was run on a computer with a 16 GB RTX 4090 GPU, which is a relatively light and common GPU that can also be used in rugged industrial PCs that are suitable for the rough CDW processing environment.

In total, the simulation has been run using four configurations with different levels of verbosity (see Table 2) on the model with an adapted, lightweight regression head: V00, V10, V20, and V01. Here, the former number refers to the verbosity of the segmentation module and the latter to that of the PSD prediction module.

Table 2. Verbosity options for processing time simulation analysis

Verbosity	Module	Description
0	Segmentation	No saving
1	Segmentation	Save metadata
2	Segmentation	Save metadata and highlighted map
0	PSD prediction	Save metadata
1	PSD prediction	Save metadata and PSD plot

2.2.4. Preliminary implications for CE Developments Implementing a new technology in a real industrial process has many implications for the CE, which range from the operational energy demand and raw material footprint of the technology to downstream application of the produced material, the company's investment ability and digitalization for e.g. material traceability. To provide insights into the impact our technical solution might have on the sector, we discuss three aspects related to the main goals of CE.

Starting with the social aspects, we assess two of the most relevant social indicators based on Padilla-Rivera et al. (Padilla-Rivera et al., 2021): labor practices — training and education, and product responsibility — product and service labeling. For training and education, we compare the hours of training with and without the implementation of the (digital) technology and determine the percentage increase. We base this approximation on the total hours of relevant training available through TÜV Nord (TÜV Nord, 2026a) and empirical estimations based on practical experiences from this case study. For product and service labeling, we base the implications on the data coverage results and relate it to the minimal necessary information for establishing a useful digital product passport (DPP) (Çetin et al., 2023; Ruismäki et al., 2025).

Given that the environmental impact of the technological system in its use phase is predominantly determined by the system's energy consumption, as part of this assessment, we determined the approximate energy demand of the pipeline. We performed this assessment on a computer with a 16 GB RTX 4090 GPU (as described in Section 2.2.3) and by utilizing the pynvml Python package for GPU demand calculations as well as a custom utilization-based approximation function to estimate the CPU demand:

$$E_{CPU} \approx \frac{P_{CPU} \cdot \Delta t}{3600}$$

with

$$P_{CPU} \approx u_{CPU,0} + \frac{u_{CPU,1} \cdot \rho_{CPU,i}}{100}$$

and

$$u_{CPU,1} = u_{CPU,TDP} - u_{CPU,0}$$

and

$$u_{CPU,0} = max(2.0, u_{CPU,TDP})$$

where E_{CPU} is the energy demand (Wh), P_{CPU} the power demand (W), Δt the time difference between the start and end of the measurement (s), $u_{CPU,0}$ the CPU demand when idle (W) with a minimum value of 2.0 W, $u_{CPU,1}$ the maximum utilizable CPU demand (W), and $u_{CPU,TDP}$ maximum utilization (W) based on the processor type (in this case Intel i7 13800H, 45 W). The total energy demand of the pipeline is determined by calculating the sum of the CPU and GPU demand.

Based on the results of the processing time simulation analysis (see Section 2.2.3), the fastest and slowest configuration were used to determine the energy demand, where both configurations were run thrice with a duration of one hour per run. The results were then analyzed and averaged per configuration to get an idea of credible energy demands for the current pipeline and utilization on a relatively small-scale processing unit. Based on the data sheets of the system's periphery — the LED light bar (0.16 kW (planistar Lichttechnik GmbH, 2026)) and the RGB sensor (0.137 kW (JAI A–S, 2025)), respectively — we could calculate the total energy demand of the quality monitoring system. For the environmental impact of the utilized energy, we consider the electricity mix and corresponding carbon intensity (342 gCO2–eq/kWh) for Germany in 2025 (Electricity Maps, 2026).

However, merely assessing the technological system in terms of its energy demand-based environmental impacts does not cover the avoided impacts associated with the application of recycled concrete in road and building construction influenced by the technological system's implementation. Given the persistent skepticism regarding the use of RA from CDW, we assume that — without the SBQM system — all RA is used for subbase layers in road construction (Tefa et al., 2022). With the implementation of the SBQM, we assume that the increased transparency about the quality of the RA will reduce this skepticism (Varli et al., 2026) and may lead to a significantly higher usage of RA in concrete for building construction. The resulting choice between road and building applications therefore requires a comparative assessment of the environmental implications of both RA utilization pathways. As such, we conducted a simplified, comparative and attributional cradle-to-gate LCA to 1) quantify the environmental impacts of RA use in road and building construction relative to their respective primary aggregate (NA) alternatives and 2) compare the resulting avoided impacts.

The LCA was conducted from the perspective of a German recycling plant comminuting CDW — the central case in this case study — which results are intended to support decisions regarding the assignment of the annual RA output to road or building construction. As visible in Figure 3, two levels of comparison are considered. First, within each application, the environmental performance of the product system with NAs and

RAs were compared (i.e. top and bottom system boundaries). Second, the environmental implications of using the annual RA output of the plant in road and building construction were compared (middle system boundary). Correspondingly, the geographical scope of the LCA is Germany. Moreover, the TRL represents current market standards except for the product system of RA in building construction, which is on a pilot plant level due to the SBQM. For the LCA, existing processes from the Ecoinvent 3.11 database (Wernet et al., 2016) were predominantly used and adapted to fit the technological and geographical scope. In the case of assignment for road construction, the corresponding process "road construction" was utilized: it starts with the production of primary, crushed gravel (i.e. NA_c), which is then transported by train and lorry to the construction site and used for road subbase stabilization. For building construction, we adapted the Ecoinvent process "concrete production, 25 MPa for building construction, with cement, CEM II/B," which requires round gravel (NA_r) to produce concrete.

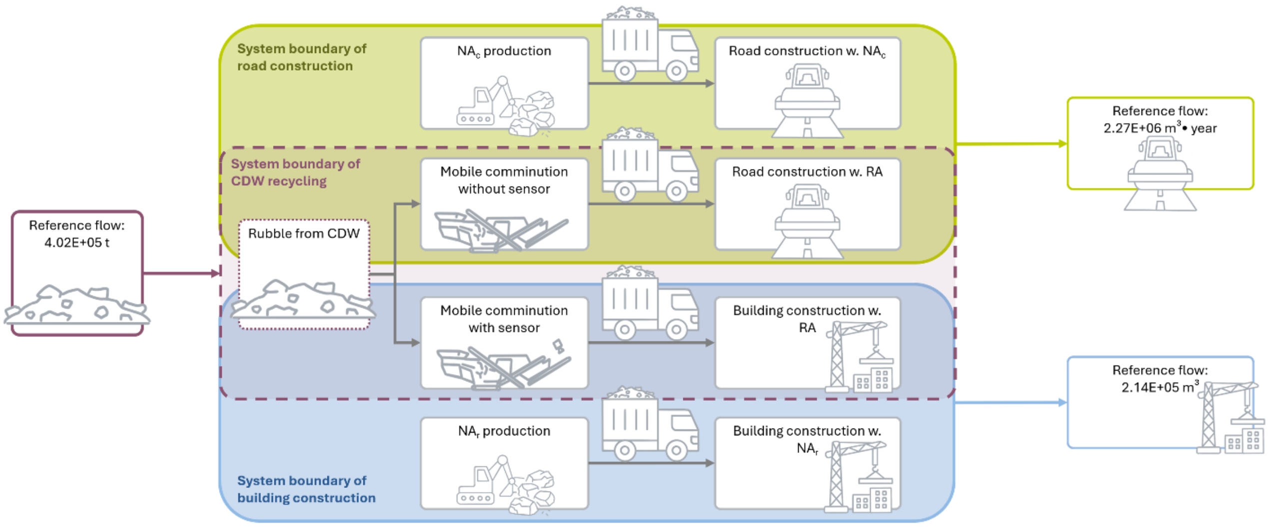

Figure 3. Flowchart of the conducted simplified, comparative cradle-to-gate LCA and corresponding system boundaries

To obtain the two product systems that recycle RA from CDW, we fully replaced NA with RA. In the product system of road construction, this implies substituting the crushed gravel by the RA, which is produced by mobile comminution (pre-sieving, crushing, and sieving). The production of one Mg RA requires 1.67 Mg rubble from the demolition process, as 40 % of this input is screened out and landfilled as inert waste. Furthermore, the comminution process consumes 13.88 MJ diesel, of which 2.75 MJ is used to load the rubble into the crusher (Fraj & Idir, 2017; Lachat et al., 2021) and 11.13 MJ to operate the machine (KLEEMANN GmbH, 2022). For the building applications, the comminution process remains similar but now includes the SBQM — approximated by a laptop with a lifetime of four years — and its energy demand (0.16 Wh/Mg RA), which is based on the previous calculation. Additionally, a further adjustment regards the water use: while the production of one cubic meter concrete with NA requires 175 kg water and 1.25 Mg NA, one cubic meter RA-concrete consumes 204 kg water and 1.13 Mg RA (Verein Deutscher Zementwerke, 2022). A detailed unit process table of both comminution processes can be found in Appendix 1.

The cut-off rule was applied, so no impacts from the construction and demolition of the original building but all impacts from the recycling process are applied to the RA. Furthermore, to resolve multi-functionality arising from the dual role of CDW, we used substitution to account for avoided emissions from keeping the CDW in the loop instead of landfilling. It should be noted that RA derived from CDW is chemically analyzed to assess the potential risk of pollutant leaching (Bisciotti et al., 2025). Since only a small sample is tested, we consider its environmental implications negligible and omit the process. Furthermore, following Ecoinvent, the mean transportation distances are assumed equal in all four product systems. The environmental impact categories considered in this work are climate change, material resources, particulate matter (PM) formation (Fantke et al., 2015), and water use. For the calculation of the category indicators, we used the EF v3.1 impact assessment method in accordance with the EU recommendations (European Commission, 2021). The impacts were calculated using the openLCA v2.6 software from GreenDelta (GreenDelta GmbH, 2026). As such, given that the assessment is a simplified LCA, it aligns with, but does not fully conform to, the ISO 14040/44 standard for life cycle assessment (International Organization for Standardization, 2006).

Three functional units (FUs) are defined: 1) for the road construction comparison, the FU is “constructing 22,273,207.55 m • year road infrastructure including maintenance over the assessed service period of one year”; 2) for the building construction comparison, “producing 214,469.06 m^3 of concrete used in building constructions”; 3) for the RA assignment comparison, “processing 401,600 Mg CDW.” To determine the FUs, a yearly output of 240,960 Mg RA is assumed, based on 200 Mg per hour production (KLEEMANN GmbH, 2022) and 8-hour operation duration for 251 days per year (C. Varli, personal communication, December 5, 2023).

Finally, for the economic implications, we determined the total costs of implementing and operating the specific system used in this case study and use literature data, particularly those presented in the discussion paper by Sterk (Sterk, 2023) as well as recent prices for different material categories in Germany (Baustoffeliefern.de, 2026; Majuntke Logistik & Umwelt, 2026). Sterk describes realistic willingness-to-pay (WTP) values for three groups of interviewees (developers, organizations, and private individuals) for different measures, of which one is the presence of a label for (recycled) concrete aggregates. This information was used to determine the additional yearly revenue that could be made solely on the additional share of labeled material provided by the quality monitoring system. Additionally, for the medium-term prospective, we investigated how a shift in application may influence the yearly revenue. This assumption is based on expert discussions that took place during the KIMBA project, where it was argued that RA with sufficient quality is instead downcycled to a lower-grade application (Varli et al., 2026) For the (additional) operating costs, we consider the energy costs needed to operate the system, based on the calculated average energy demand and the average yearly energy costs (€89.33/MWh) for Germany in 2025 (Bundesnetzagentur, 2026; Electricity Maps, 2026).

3. Results

3.1. Recording constancy

To investigate the fluctuations during execution of the campaign as well as to compare these fluctuations on different occasions within the year, we conducted different statistical tests performed a visual comparison.

First, the ACF was plotted for each experiment. Visual inspection of these plots, which are presented in the Appendix 2, indicates short-range dependence (i.e. significant autocorrelation) for experiments A1 (lags 1–2), B2 (lags 1–3), and C (lags 1–2). All other ACF plots do not indicate the presence of autocorrelation.

Even though the ACFs allow interpretation of the stationarity of the time series, we assessed this separately by performing the ADF test. These results are presented in Table 3. This assessment indicates that stationarity is supported at the 5 % significance level for most experiments. There are seven time series where no stationarity can be assumed at the 5 % level: A1, A3, A4, A7, B2, B3, and B6. This coincides with our visual inspection of the time series: A1, A4, A7 and B3 show some negative drift over time. Additionally, there are visible irregularities with clearly distinguishable valleys for A1, A3, A7, B2, and B6, particularly towards the end of each series. For B2, the source of the irregularity is known, as there was a power outage after around six minutes. This is visible in the time series plot. These plots are available for each experiment in the Appendix 3. The ADF test’s conservative nature means that seven cases are identified as potentially non-stationary, but further inspection confirms that only four experiments exhibit persistent drift. Furthermore, these results indicate that acquiring strong stationarity is not trivial given the rough conditions, but is nonetheless achieved for most experiments and, in particular for the experiment with the longest recording duration (C), where the ADF result is most informative given its lower power for shorter series.

Table 3. Results of the ADF test. Abbreviations: ADF = Augmented Dickey–Fuller; CV = critical value

Experiment ID	ADF statistic	p-value	CV 1 %	CV 5 %	CV 10 %	Stationary at 5 % level
A1	-0.86	0.80	-3.68	-2.97	-2.62	
A2	-3.92	<0.01	-5.35	-3.65	-2.90	✓
A3	-1.62	0.47	-3.81	-3.02	-2.65	
A4	-0.46	0.90	-4.94	-3.48	-2.84	
A5	-3.63	<0.01	-4.14	-3.15	-2.71	✓
A6	-5.10	<0.01	-3.68	-2.97	-2.62	✓
A7	-2.80	0.06	-3.68	-2.97	-2.62	
B1	-3.26	0.02	-3.71	-2.98	-2.63	✓
B2	-1.52	0.53	-3.64	-2.95	-2.61	
B3	-2.73	0.07	-3.89	-3.05	-2.67	
B4	-3.13	0.02	-3.89	-3.05	-2.67	✓
B5	-3.74	<0.01	-3.74	-2.99	-2.64	✓
B6	-0.52	0.89	-3.74	-2.99	-2.64	
B7	-5.42	<0.01	-3.81	-3.02	-2.65	✓
C	-3.42	0.01	-3.54	-2.91	-2.59	✓

In Figure 4, an overview of the frequency distribution for all experiments is provided, which shows overall high similarity between the sets of experiments. The difference in median between the different sets stems from re-calibration of the acquisition speed settings in the camera, which were adjusted to better match the speed of the conveyor belt. Furthermore, it can be seen that B1 has particularly narrow bounds (i.e. low variation), which matches the previous statistical findings. Similarly, A1 and B2, in particular, are in line with the interpretations from the statistical tests and show high variance. For B2, the influence of a power outage on the variance is clearly indicated: the overlay boxplot — where all values within the time range of the power outage are removed — shows narrower bounds and a slightly higher median. Finally, the resulting distribution for experiment C is important, as this is the demo experiment where data have been recorded without interruption during a longer time period compared to the other experiments. It can be seen that the bounds remain small, indicating recording stability for this duration.

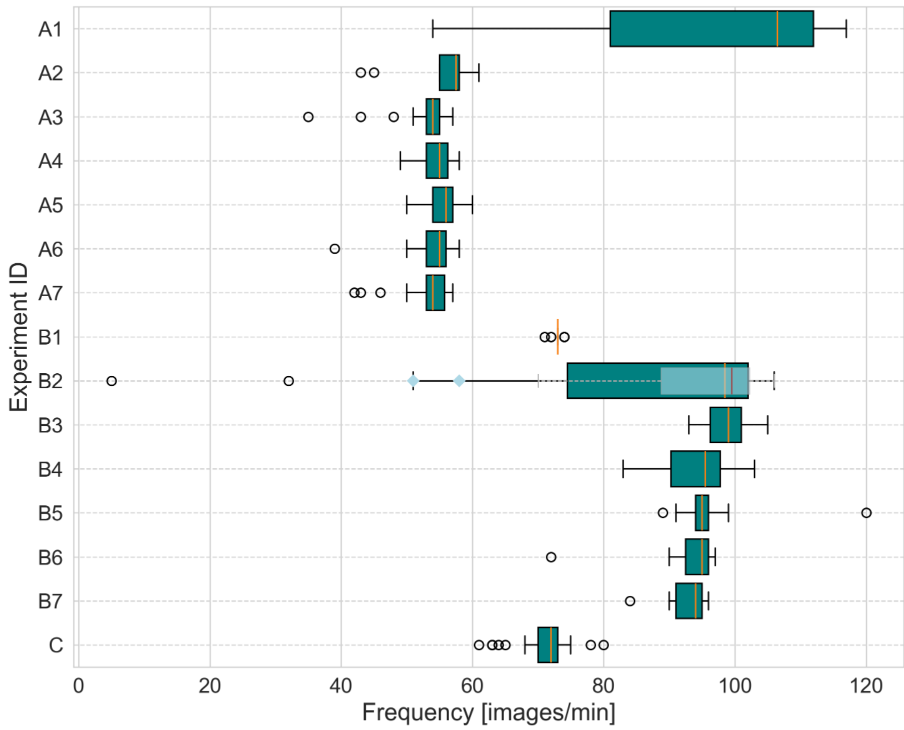

Figure 4. Horizontal boxplot of the recording frequency distribution for each experiment. For B2, a light blue overlay is added, which contains the information when ignoring the values during the power outage. Red and orange bars: median; boxes: interquartile range (IQR); whiskers: data points within 1.5 times the IQR; circles/diamonds: outliers.

With Levene's test for equality of variances, we have assessed whether the variance for the sets of experiments is equal on the 95 % confidence level. In Table 4, the results are shown. If the p-value is lower than 0.05, it means that there is proof for non-equality of the variances. As such, it is a weak indicator for equality of the variances from the respective sets in the case of $p \geq 0.05$. As indicated in the methods, severe irregularities have also been removed. More specifically, for A, experiment A1 has been excluded due to the large fluctuations (see also Figure 4). Similarly, for B, experiment B2, which contains the power outage interruption, has been excluded entirely. All other time series have not been adjusted to avoid confounding or misleading results. For most of the sets, in particularly those with seemingly spurious time series (A1 and B2) removed, non-equality cannot be assumed. This indicates that generally, fluctuations in the recording frequency are similar during the course of a day (row 1 and 2) and on different days across the year (row 6–8 and 10).

Table 4. Results of the Levene test for equal variances. Abbreviations: RT = random test (permutation-based); A = experiment A1–A7, A_{adj} = experiment A2–7; B = experiment B1–B7, B_{adj} = experiment B1, B3–B7; C = experiment C

Row	Set ID	Levene statistic	p-value (RT)	p-value	Equality possible?
1	(A_{adj})	0.62	0.69	0.68	✓
2	(B_{adj})	1.80	0.11	0.14	✓
3	(A, B)	2.55	0.10	0.11	✓
4	(A, C)	10.70	<0.01	<0.01	
5	(B, C)	14.98	<0.01	<0.01	
6	(A_{adj}, B_{adj})	1.30	0.25	0.26	✓
7	(A_{adj}, C)	0.50	0.48	0.48	✓
8	(B_{adj}, C)	2.37	0.13	0.13	✓
9	(A, B, C)	8.02	<0.01	<0.01	
10	(A_{adj}, B_{adj} , C)	1.44	0.22	0.24	✓

3.2. Data Coverage

For an estimation of the data coverage, three models were used to analyze the images corresponding to samples 1 and 2 of set C. Each model has different sensitivities towards the different classes, which allows the calculation of a conservative average coverage, as well as best and worst cases. The results of these calculations are presented in Figure 5. The relative coverage is similar for both experiments (or samples), for all classes except 45–63 mm. The latter class also suffers from large variation in the relative coverage due to high or full insensitivity by some of the models and high sensitivity by others. Additionally, there is low coverage for particles in the class 31.5–45 mm by all three models, which corresponds to the results presented in our previous study (Göbbels et al., 2026), where a relatively large classification error (i.e. ~50 % switched between 31.5–45 mm and 45–63 mm) for this class was present.

Overall, the micro-average coverage of the models is 8.6 % and 7.9 % for particles ranging from 4 mm to 63 mm, respectively, when aggregating the true sample weight and the predicted weight for each analyzed instance. Interestingly, for both samples, the micro-average is similar, with a slightly lower %–coverage by weight for sample 2. This corresponds with the slight difference in the total weights of the samples: 212.1 kg (sample 1) and 223.5 kg (sample 2). However, besides the particles in the range 4–63 mm, there is also a fine fraction, which has thus far not been taken into account, as the segmentation model is unable to identify particles smaller than 4 mm. The remaining fine fraction corresponds to 73.6 kg or 34.7 % for sample 1 and 73.2 kg or 32.8 % for sample 2. When including the fine fractions into the calculation of the coverage, it would mean that 5.6 % and 5.3 % are covered, respectively.

Given the latter micro-averages and assuming an average production of 200 Mg/h input and 120 Mg/h output for eight hours a day and five days a week based on empirical values, it would mean that approximately 51–54 Mg of output material can be monitored each day, accumulating to 254–269 Mg each week. Given that around 80 kg are manually sampled each week, the yearly weight of material that is covered in addition to the manual sampling sums up to around 13.2–14.0 kilotons.

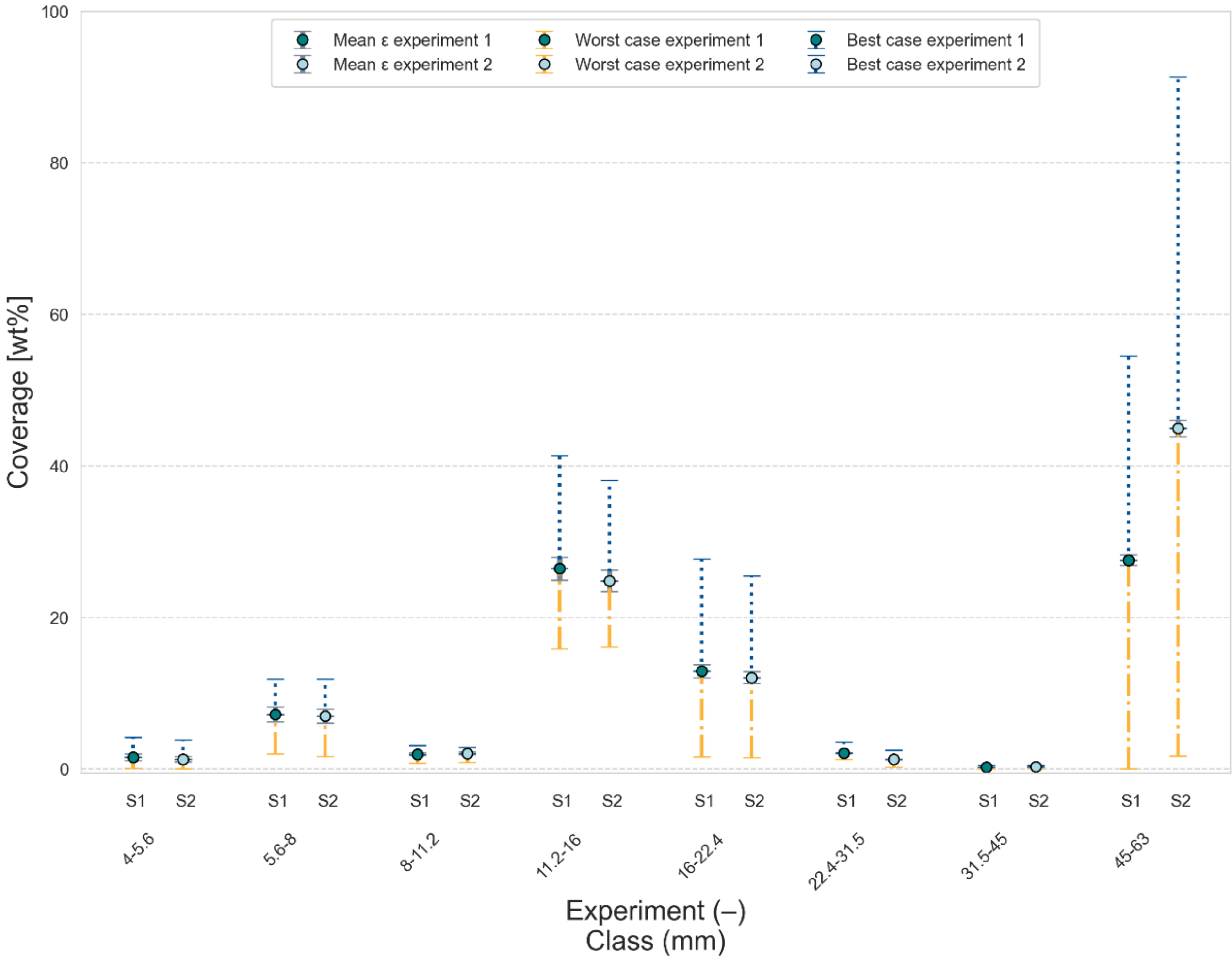

Figure 5. Plot for the visualization of approximate data coverage in terms of wt% of the material flow (based on samples C1 and C2). Abbreviations: ε = error; S1 = sample C1; S2 = sample C2.

3.3. Processing Time

For the processing time, both the mean and median have been calculated after letting the simulation iterate through 296 images for each verbosity configuration. The results are presented in Tables 5 and 6. It can be seen that the processing time for the procedures not affected by changes in verbosity (i.e. model loading and analysis), remain stable across all four simulations, with the exception of one outlier value during V10: here, both the segmentation and PSD prediction module went idle without shutting off, leading to one image taking 5,500 s to be analyzed. Since this was the only occurrence of idling, an adjusted mean — without the outlier — is also provided. Loading ParticleSAM at the start of the segmentation takes around 0.8 s and the identification of the instances generally takes around 18 s. However, given the many instances per image, for which the masks need to be generated as well as processed and saved for the subsequent model, the data processing and saving procedure in the segmentation module takes nearly two minutes at the minimum. When increasing the verbosity, i.e. saving additional information, this results in an increase of around 5 s for metadata saving and around a minute when saving both the metadata as well as a highlighted map, which is necessary for direct visual assessment of the segmentation results. The processing time of the PSD prediction module is clearly lower, with around 6 s for the entire AI-based PSD prediction procedure and 14 ms for saving of the results. Interestingly, there are no clear increases here when increasing the verbosity, i.e. when additionally saving a graphic of the predicted PSD.

A similar trend is also visible for the median, which is calculated to provide results that are more robust to outliers. The median values are slightly lower and even more stable compared to the mean values, but show the same trend: high stability across configurations with around 5 s increase when saving segmentation metadata and around a minute additional processing time when saving both the highlighted map and the metadata in the segmentation module. Summing the results for the fastest configuration (V01) and the slowest (V20) leads to a mean range of 137.4–214.8 s and a median range of 134.8–209.3 s. So, with the current pipeline, it is feasible to provide a new PSD every four minutes in a live monitoring context. Besides the live monitoring, images that are being recorded during processing can be stored separately in parallel, for instance for delayed at-line analysis.

Table 5. Mean processing time (s) for each procedure in the main modules, segmentation and PSD prediction. Abbreviations: V = verbosity; (00, 10, 20, 01) = verbosity configurations, where the first number refers to segmentation verbosity and the last number to the PSD prediction verbosity (see also Table 2); adj. = adjusted, value after removing outlier.

Configuration	Segmentation			PSD Prediction	
	Loading model	Analysis (adj.)	Saving	Analysis (adj.)	Saving
V00	0.774	18.633	120.711	6.258	0.014
V10	0.794	36.580 (17.750)	125.102	24.561 (5.761)	0.014
V20	0.850	18.729	188.879	6.373	0.014
V01	0.793	17.963	112.879	5.785	0.014

Table 6. Median processing time (s) for each procedure in the main modules, segmentation and PSD prediction. Abbreviations: V = verbosity; (00, 10, 20, 01) = verbosity configurations, where the first number refers to segmentation verbosity and the last number to the PSD prediction verbosity (see also Table 2)

Configuration	Segmentation			PSD Prediction	
	Loading model	Analysis	Saving	Analysis	Saving
V00	0.763	16.345	119.926	5.284	0.014
V10	0.770	16.480	124.151	5.326	0.013
V20	0.816	16.823	186.423	5.212	0.013
V01	0.774	16.633	112.182	5.192	0.014

3.4. Preliminary implications for CE Developments

To get a preliminary idea of the social impacts the technology may have, we focus on two specific aspects: training, and product labeling. Moreover, we included PM formation as one of four investigated environmental impact categories in our LCA. This category is directly linked to downstream health effects, given that PM is one of the main contributors to the global human disease burden. These results are presented in Figure 6(b) and discussed in the corresponding paragraph. For the first aspect, we identified a total of 8 work days per year of basic and recurrent training that are specifically relevant for workers on recycling plants based on the available courses on TÜV Nord (TÜV Nord, 2026a). We assume instructions on handling the new system, including learning to interpret the results, would take approximately one day, which coincides with a similar course (“Einführung Data Science”) provided by TÜV Nord (TÜV Nord, 2026b), which also takes one day. This would mean there is a 12.5 % increase in training, given that previous training cannot be reduced.

For the product labeling that stems from increased transparency on the material quality, we utilize two proposed DPPs for construction and concrete products, which is the work that comes closest to high-grade applications for the produced RC material. Ruismäki et al. (Ruismäki et al., 2025) identify four main categories, with in total 15 subcategories. Çetin et al. (Çetin et al., 2023) list six main categories with 48 subcategories. This makes it possible to calculate a plausible range of additional information, since in both DPPs, information on product properties is included. As the PSD is only a part of the product’s properties, we use DIN EN 13242 (Deutsches Institut für Normung e.V., 2008) to determine the exact share of properties the PSD covers: in total there are 13 characteristics that need to be determined, of which the PSD is one. Taking into account the data coverage (5.3-5.6 %), the share the PSD covers in terms of properties (7.7 %), and the share of particle properties in both versions of the DPP (assuming equal importance), leads to an approximate additional information availability of up to 0.1 % on the DPP level when taking only the category product properties or product data into account. Although this increase is minimal, it indicates that even having information on merely 5 % of the material stream for one quality factor has impacts on downstream information availability.

For the environmental implications of the SBQM system itself, we focus mostly on the energy demand during the use phase and refer to the detailed study of Falk et al. (Falk et al., 2026) for information on the additional impacts through manufacturing and the EoL phase, which should be taken into account during the decision-making process of implementing such technology. The results of the simulation analysis (see Section 2.2.4), are described in Table 7, which shows the average energy demand for each of three runs for the two selected configurations. Using the global average (19.23 Wh), the total hourly average energy consumption would sum to 0.316 kWh. Assuming 251 work days and 8 hours of operation per day, the total average energy consumption in one year would be 635 kWh for the entire system. This would equal a carbon footprint of 217 kgCO2–eq. per year.

Table 7. Mean energy demand (Wh) for each simulation. Abbreviations: V = verbosity; (00, 20) = verbosity configurations, where the first number refers to segmentation verbosity and the last number to the PSD prediction verbosity (see also Table 2).

Run	Total energy demand (Wh)	
	V00	V20
1	19.59	17.07
2	21.01	16.38
3	22.93	18.40
Mean	**21.18**	**17.28**

The results of the environmental implications based on the LCA are presented in Figure 6. For both applications, the environmental impacts associated with the utilization of NA are always higher than for RA. So, regardless of assignment, the deployment of RA has the potential to avoid emissions for each assessed impact category. For both applications, the biggest impact reduction is for water use: 18 million cubic meters (61 %) for building and 5 million cubic meters (58 %) for road construction (see Figure 6(b)). This can be explained by the considerable amount of water required during mining and production of NA (gravel).

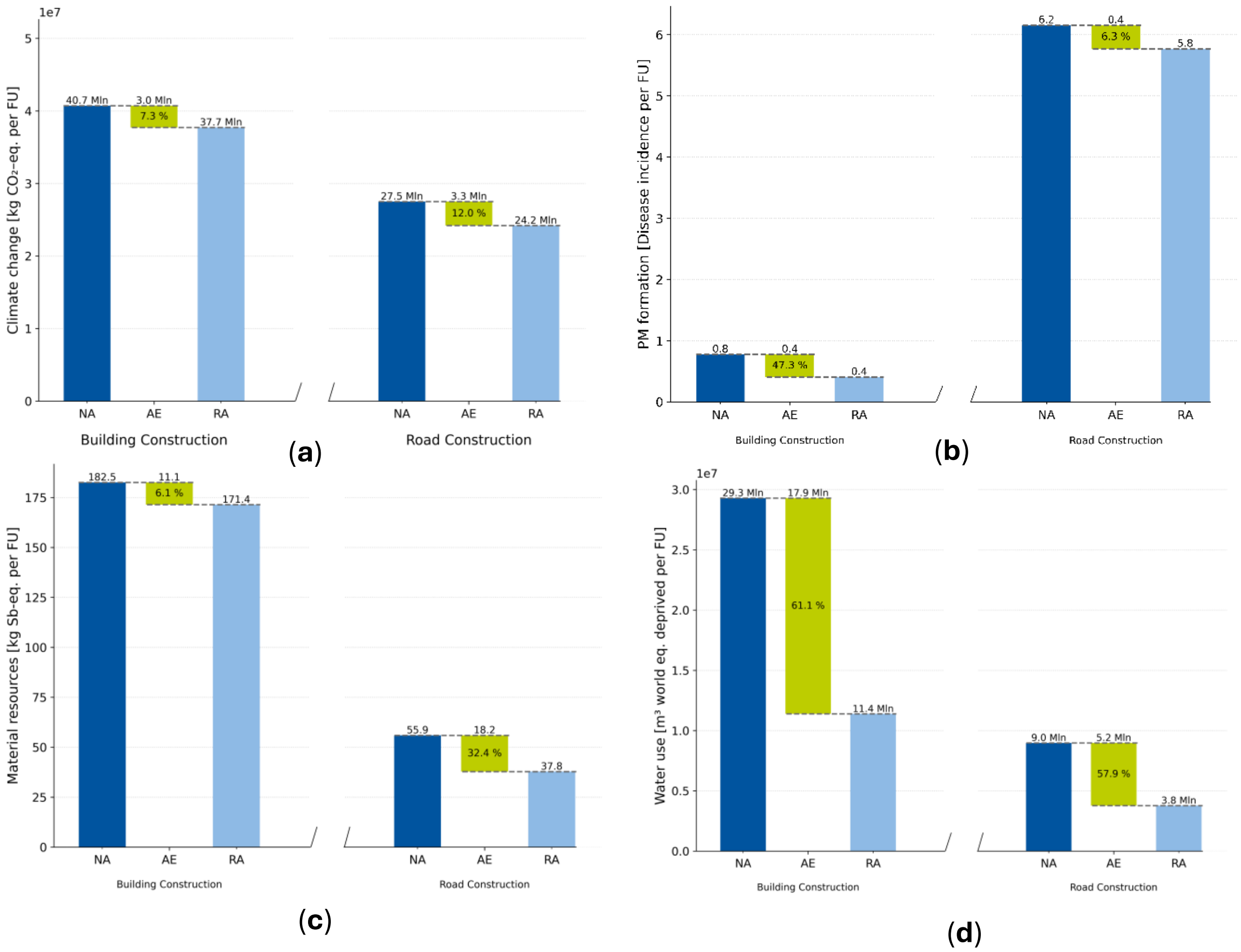

Figure 6. Bar charts with the emissions and corresponding avoided emissions when utilizing RA. (a) Climate change emissions and avoided emissions expressed as kilograms CO2-equivalent per functional unit. (b) PM formation emissions and avoided emissions expressed as disease incidence per functional unit. (c) Material resources emissions and avoided emissions expressed as kilograms Sb-equivalent per functional unit. (d) Water use emissions and avoided emissions expressed as cubic meters world equivalent deprived per functional unit. Abbreviations: FU = functional unit; NA = with natural aggregates; AE = avoided emissions; RA = with recycled aggregates.

When comparing the impact reduction potential of RA in absolute terms, utilizing RA in road construction has a slightly larger potential for reduction in all categories except water use, which can be partially explained by the additional electricity required for the SBQM system during production of RA for building construction. However, when comparing the relative potentials, RA in building construction leads to higher relative reduction of PM formation: 47 % compared to 6 %. This difference reflects the higher baseline PM impacts of road construction. This result is also relevant for the social dimension: (fine) particulate matter is a major environmental factor that contributes to global human disease burden, so lower PM formations through the use of RA may have direct effects on downstream employee or consumer health. Furthermore, the RA assignment comparison indicates that RA and NA production are not the main contributors to, in particular, the climate change and material resources impacts associated with building construction.

For an indication of the economic impacts, we focus on two scenarios that implementation of the SBQM system may lead to in the medium-term: 1) additional WTP values for the larger share of material that contains a specific label, and 2) higher selling price due to the material being sold for higher-grade applications. In both scenarios we take into account the one-time payment to buy the system components, totaling € 26,000 (net costs, own information), as well as the additional energy costs to operate the system. Given 251 work days and assuming 8 hours of operation per day, the total average energy costs would sum to €56.68 for a year.

For the two scenarios we calculated best and worst cases in terms of yearly revenue based on a total production of 120 Mg/h for 8 hours per day and 251 days per year given the available data. For the first scenario, we have calculated the approximate coverage (see Section 3.2), which we keep as fixed value.

Instead, we use the lowest and highest WTP value described by Sterk (Sterk, 2023) to acquire a plausible range. That is, the lowest WTP is +€11.33/m^3 (lower limit for developers) whereas the highest WTP equals +€28.33/m^3 (upper limit for developers). WTP values for organizations and private individuals all fall within these bounds. Since our calculations are based on product weight, instead of volume, we utilize the corresponding assumption of €150/m^3 for concrete as average price (Sterk, 2023). This would mean that the price increase lies between 7.6 % and 18.9 %. Assuming a similar price increase is back-calculated to the selling of the RA, currently priced at around €6.05/Mg (Baustoffeliefern.de, 2026; Majuntke Logistik & Umwelt, 2026), a yearly additional revenue of €6,069–€16,008 may be possible given the additional share of labeled material. The former value stems from multiplying the lowest yearly coverage (13.2 kilotons) with the lowest price increase (7.6 %) and the latter from multiplying the highest yearly coverage (14.0 kilotons) with the highest price increase (18.9 %).

For the second scenario, we use the detailed price list of Baustoffe-liefern (Baustoffeliefern.de, 2026) as best case, where an overview of all mineral material types including prices across Germany in 2026 is provided. The status quo of our case study is $G_{B,0/45}$ or "RCL I 0/45", a lower-grade product which is priced at €6.05/Mg. With increased transparency due the quality monitoring system, the material may instead be sold as the higher-grade option "RCT 0/45" at €15.71/Mg. However, as is also visible from the many options in the aforementioned source, it should be taken into account that prices fluctuate across geographical locations and time, partially due to material availabilities. Additionally, it should be noted that better monitoring of the PSD alone may not be enough: data on chemical, mechanical and further regulatory compliance may be necessary (Müller, 2018), which can lead to increases in processing costs of RA for the highest-grade applications. When using the price increase of €9.66/Mg, it would mean that an additional total yearly revenue of €127,512–€135,240 could be achieved. The calculations based on WTP are more conservative, but seemingly closer to real scenarios. Even in the case of acquiring additional yearly revenue of around €6,000, it means that there is a return on investment of the system within approximately 4.5 years.

3.5. Limitations and Future Work

3.5.1. Recording Constancy In terms of recording constancy, it should be noted that the use of a line scan sensor poses some limitations to the interpretability of the results. Even though we have not used an encoder to automatically match the line scanning frequency to the speed of the conveyor belt, which is advantageous for independent recording frequency assessment, manual adjustments have taken place to better match the frequency and get higher-quality image recordings, as this was the main priority during the experiments. These differences are, however, clearly visible between the experiment sets. Nonetheless, the overall results indicate recording stability for most of the experiments, even when this aspect was not the main focus. Further optimization of the stability can be achieved by adjusting the field of view (FOV): in the case study, the sensor was always recording at full resolution, partially recording non-moving parts of the conveyor, as well as saving the image data in a heavy, non-compressed file format. Later investigations however resulted in the finding that the FOV for this particular plant can easily be reduced to half the width without compromising valuable parts of the image and that saving with minimal compression in a different format significantly reduces the memory occupation without going below the minimal resolution necessary for subsequent processing.

3.5.2. Data Coverage The results provide first insights into the share of material being analyzed by the pipeline, however, more research is necessary in this regard. For instance, the current values, in particular between best and worst case, diverge significantly, which hampers the determination of weighing factors for each class to come to a final PSD that closely approximates the entire material flow, instead of just the top layer. Moreover, the low sensitivity for class 31.5–45 mm suggests the need for further performance optimization of the models, especially in the context of larger imaging distortions of the (bigger) particles due to external influences such as the significant machine vibrations. For instance, on the basis of statistical process control, a warning system to avoid heavily distorted images entering the processing pipeline could be developed. This is an important aspect for many AI-based processing pipelines, as neural networks inherently lack robustness and are thus susceptible to even minor input perturbations (König et al., 2024; Szegedy et al., 2013). Furthermore, since no new model performance assessment was conducted in the present study, relevant insights could be acquired when validating the performance of an optimized version of the model in an industrial setting. Additionally, likewise, further research should focus on the error propagation between modules and on the validation of the segmentation module in an industrial context in particular, since it may well be that there are errors in segmenting the particles belonging to e.g. the class 31.5–45 mm.

Moreover, the presence and share of fine fraction classes are relevant topics for the industry but have been largely ignored in this study due to the impossibility of the segmentation model to identify these smaller particles. For future research, investigating the potentials of adding an additional sensor, for instance with a different zoom configuration — this is possible on the currently used RGB since it has sufficient resolution, to monitor the fine fraction in parallel, would be relevant. This would allow the use of the processing pipeline, but with different calibration factors or even with a specially adjusted PSD module to adjust for the change in spatial resolution. Additionally, a parallel system adjusted for fine fraction monitoring could be positioned on the fine fraction output conveyor directly after pre-sieving to potentially optimize the recycling for this specific fraction. Even though larger coverage is desired, having continuous monitoring of the largest size fractions may nonetheless already be valuable for more timely identification of problematic changes regarding these fractions and corresponding adjustment of the machine parameters or input composition. The experiment campaigns conducted in this case study indicated that granular convection occurs on the output conveyor, which suggests that many large particles are visible to the SBQM system, but further research is required to investigate actual correlations between the monitored top-layer share of the stream and the full output stream. In this regard, it is also interesting to investigate generalizability, which could not be assessed in this work due to its case study nature.

3.5.3. Processing Time In terms of processing time, the relatively heavy-weight segmentation module turns out to be the main bottleneck, limiting the monitoring to 4-minute sampling intervals. Even though this frequency is sufficient for current industry demands, for instance in the context of adaptive process control, it should be optimized further for adequate live coverage. Alternatively, investigations could focus on fluctuations in the material stream — in particular the top layer, as this is being recorded — to determine adequate intervals. Nevertheless, looking at the remaining components and the differences of low and high verbosity settings, processing times remain stable across configurations and modules. Especially interesting is the low analysis duration for the two models given the high-resolution and particle-dense images: 16 and 5 seconds (median) for the segmentation and PSD prediction models, respectively.

3.5.4. Preliminary implications for CE developments With respect to the identified implications for CE developments, we would like to highlight that these are merely preliminary indications of the positive and negative aspects the quality monitoring system may have upon implementation in practice. For a more exhaustive view, conducting further analyses such as a holistic life cycle sustainability assessment (LCSA) is essential. However, given that the scope of the case study has been to post-hoc describe the technical aspects of implementing the developed system while at the same time taking into account the broader aspects of CE, it was infeasible to systematically execute an exhaustive LCSA or the like.

Even though many relevant social impact indicators are described in literature (e.g. (Padilla-Rivera et al., 2021)), it was only possible to estimate two of them given the data available to us from this case study. Even though the indicators regarding employee training and product labeling show slightly positive impacts, it is not enough to draw solid conclusions on the overall social impacts. For instance, the consumer health and safety has not been taken into account as an indicator, but is relevant in the wider context of using RA for road or building construction (Padilla-Rivera et al., 2021) when relying more on the results of the monitoring system instead of frequent, but labor-intensive manual sampling. Such trade-offs can be a consideration for future social-LCA-focused investigations.

Similarly, for the environmental aspects, the sector would benefit from an exhaustive LCA with more detailed scenario analyses, especially in the context of Germany's EBV, which further regulates the production and application of RA from CDW (Bundesministerium für Umwelt, Klimaschutz, Naturschutz und nukleare Sicherheit, 2023). Moreover, since environmental impacts for CDW are highly dependent on transport and the substitution potential (Bayram et al., 2025), we consider performing a more detailed LCA beneficial. In addition, the present LCA assumes all RA produced with the support of SBQM can be used in concrete production, which may not be realistic as suitability of the material depends on additional properties such as eluate concentrations. Future analyses should therefore account for the share of RA meeting all relevant quality requirements. Combining these sector-specific aspects with the frequently-overlooked cradle-to-grave impacts of high-end technology (Falk et al., 2026) such as GPUs, industrial PCs, but also advanced sensor systems, may provide relevant new insights on the environmental trade-offs embedded in the implementation of new technology.

For holistic cost analysis, life cycle costing or similar modeling approaches should be conducted to get a more exhaustive view of the actual economic impacts. For instance, due to the post-hoc assessment with limited information, we have restricted ourselves to mostly literature data as well as price increase scenarios that may not easily occur in practice or are bound to additional costs, such as further laboratory tests for added chemical quality factors for high-grade products. However, both findings in literature as well as from this case study indicate that higher transparency and an increase in information about the material quality increases the consumer's willingness to pay and trust in the product (Bellini & Bang, 2022; Osei-Tutu et al., 2023; Sterk, 2023). So, it is safe to argue that there is value in closing the information gap of true material quality.

4. Conclusions

In this work, we show that the developed quality monitoring system prototype contributes to data availability in the context of monitoring material on the discharge conveyor of a mobile CDW comminution unit. Our investigations on recording constancy, data coverage and processing time show overall promising results, but further room for optimization remains. With stationarity and high probability for equal variances for most experiments, data acquisition has turned out to be generally robust, even in the demanding environment while operating the sensor at full resolution throughout the experiments. In terms of data coverage, a clear increase in the monitored share of the material stream is possible compared to the manual sampling-based procedure, but further research is necessary to identify ways to make valid estimations of the entire stream. This also includes an industrial implementation performance validation study for the used prediction model, which is considered out of scope in this work. The segmentation module suffers from long processing time compared to the other modules, but this can be explained by the heavy data load embedded in the processing of the identified particles for the subsequent module. Given the current industry demands, the resulting interval of 4 minutes is deemed sufficient for a range of applications, such as adaptive process control, but should be improved for true live monitoring.

A first set of preliminary implications for the CE is provided by addressing several social, environmental and economic aspects. With slightly positive impacts on employee training and a minor increase in information for downstream DPPs, both investigated social aspects give a weakly positive view. For the environmental aspects, the use of RA provides environmental benefits in both road and building construction across all considered impact categories. The relative reduction potential, however, differs between applications: RA deployment in road construction achieves bigger reductions in climate change and material resource impacts (12 % and 32 %, respectively), whereas deployment in building construction offers more prominent reductions in water use (61 %). The investigated scenarios on the potential economic impacts suggest that such investments may be economically viable under the assumptions considered, particularly if increased transparency leads to additional revenues without substantial additional (laboratory) testing or processing costs. Moreover, similar results can probably be achieved by an RGB sensor with lower resolution, which may lower the investment costs significantly. So, in this work, we provide a multi-faceted analysis of the developed SBQM system for monitoring the PSD during CDW comminution, which has been implemented in a real CDW processing environment on a full-scale mobile comminution machine. This analysis shows the potential of our system in the context of the CE and may provide vital insights that support the transitioning towards a circular and sustainable construction sector.

Acknowledgements The authors would like to extend their appreciation to the KIMBA consortium, comprising MAV Krefeld GmbH, KLEEMANN GmbH, DFKI, Universität Siegen and Point8 GmbH, for supporting this study.

Author Contributions Lieve Göbbels: Conceptualization, methodology, software, validation, formal analysis, investigation, resources, data curation, writing–original draft preparation, writing–review and editing, visualization. Dietlind Ahrens: methodology, software, formal analysis, investigation, writing–review and editing, visualization. Karoline Raulf: Conceptualization, writing–review and editing, supervision, project administration, funding acquisition

Funding This work was funded by the German Federal Ministry of Education and Research (BMBF), now the German Federal Ministry of Research, Technology and Space (BMFTR), within the program "Digital GreenTech" under the project KIMBA (grant no. 2WDG1693D). Open access funding was provided by the RWTH Aachen University Open Access Publication Fund. The responsibility for the content of this publication lies with the authors.

Data Availability The datasets presented in this article are not readily available because the data are part of an ongoing study. Requests to access the datasets should be directed to the corresponding author.

Declarations

Competing Interests The authors declare no competing interests.

References

Alhawamdeh, M., Ferriz-Papi, J. A., & Lee, A. (2024). Examining the Drivers to Support Improved Construction and Demolition Waste Management for a Circular Economy: A Comprehensive Review Using a Systematic Approach. *Sustainability*, *16*(14), 6014. https://doi.org/10.3390/su16146014

Antunes, A., Silvestre, J., Costa, H., Carmo, R. D., & Júlio, E. (2024). Reducing the environmental impact of the end-of-life of buildings depending on interrelated demolition strategies, transport distances and disposal scenarios. *Journal of Building Engineering*, *82*, 108197. https://doi.org/10.1016/j.jobe.2023.108197

Backes, J. G., & Traverso, M. (2021). Application of Life Cycle Sustainability Assessment in the Construction Sector: A Systematic Literature Review. *Processes*, *9*(7), 1248. https://doi.org/10.3390/pr9071248

Baustoffeliefern.de. (2026, June 7). *Unverbindliche Preisliste Juni 2026 aus exemplarischen Shops in Deutschland*. https://www.baustoffe-liefern.de/Schotter/Preisliste-Schotter.html

Bayram, B., & Greiff, K. (2023). Life cycle assessment on construction and demolition waste recycling: A systematic review analyzing three important quality aspects. *The International Journal of Life Cycle Assessment*, *28*(8), 967–989. https://doi.org/10.1007/s11367-023-02145-1

Bayram, B., Greiff, K., Gerlich, L., Luthin, A., Hildebrand, L., & Traverso, M. (2025). Environmental and economic implications of selective demolition and advanced recycling of construction waste. *Sustainable Production and Consumption*, *57*, 61–79. https://doi.org/10.1016/j.spc.2025.05.007

Bellini, A., & Bang, S. (2022). Barriers for data management as an enabler of circular economy: An exploratory study of the Norwegian AEC-industry. *IOP Conference Series: Earth and Environmental Science*, *1122*(1), 012047. https://doi.org/10.1088/1755-1315/1122/1/012047

Bisciotti, A., Brombin, V., Song, Y., Bianchini, G., & Cruciani, G. (2025). Classification and predictive leaching risk assessment of construction and demolition waste using multivariate statistical and machine learning analyses. *Waste Management*, *196*, 60–70. https://doi.org/10.1016/j.wasman.2025.02.033

Blackledge, J. M. (2005). Statistical Modelling and Analysis. In *Digital Image Processing* (pp. 512–540). Elsevier. https://doi.org/10.1533/9780857099464.4.512

Bocken, N. M. P., De Pauw, I., Bakker, C., & Van Der Grinten, B. (2016). Product design and business model strategies for a circular economy. *Journal of Industrial and Production Engineering*, *33*(5), 308–320. https://doi.org/10.1080/21681015.2016.1172124

Bundesministerium für Umwelt, Klimaschutz, Naturschutz und nukleare Sicherheit. (2023). *Verordnung der Bundesregierung—Verordnung zur Änderung der Ersatzbaustoffverordnung und der Brennstoffwechsel-Gasmangellage-Verordnung*. https://www.bundesumweltministerium.de/gesetz/verordnung-zur-aenderung-der-ersatzbaustoffverordnung-und-der-brennstoffwechsel-gasmangellage-verordnung

Bundesnetzagentur. (2026, January 5). *Bundesnetzagentur publishes 2025 electricity market data*. Bundesnetzagentur. Bundesnetzagentur. https://www.bundesnetzagentur.de/SharedDocs/Pressemitteilungen/EN/2026/20260104_SMARD.html

Çetin, S., Raghu, D., Honic, M., Straub, A., & Gruis, V. (2023). Data requirements and availabilities for material passports: A digitally enabled framework for improving the circularity of existing buildings. *Sustainable Production and Consumption*, *40*, 422–437. https://doi.org/10.1016/j.spc.2023.07.011

Chang, C., Di Maio, F., Bheemireddy, R., Posthoorn, P., Gebremariam, A. T., & Rem, P. (2025). Enhancing quality inspection efficiency and reliability of unscreened recycled coarse aggregates (RCA) streams using innovative mobile sensor-based technology. *Developments in the Built Environment*, *21*, 100611. https://doi.org/10.1016/j.dibe.2025.100611

Deutsches Institut für Normung e.V. (2008). *DIN EN 13242 Aggregates for unbound and hydraulically bound materials for use in civil engineering work and road construction* (13242:2008-03). Beuth Verlag GmbH.

Deutsches Institut für Normung e.V. (2018). *Unbound mixtures Specifications; English version EN 13285:2018* (13285:2018-10). DIN Media GmbH. https://doi.org/10.31030/2582545

Di Maria, A., Eyckmans, J., & Van Acker, K. (2018). Downcycling versus recycling of construction and demolition waste: Combining LCA and LCC to support sustainable policy making. *Waste Management*, *75*, 3–21. https://doi.org/10.1016/j.wasman.2018.01.028

Di Maria, F., Bianconi, F., Micale, C., Baglioni, S., & Marionni, M. (2016). Quality assessment for recycling aggregates from construction and demolition waste: An image-based approach for particle size estimation. *Waste Management*, *48*, 344–352. Scopus. https://doi.org/10.1016/j.wasman.2015.12.005

Electricity Maps. (2026). *Germany 2025 Electricity prices* [Dataset]. Electricity Maps Data Portal. https://app.electricitymaps.com/map/zone/DE/all/yearly

European Commission. (2021). Commission Recommendation (EU) 2021/2279 of 15 December 2021 on the use of the Environmental Footprint methods to measure and communicate the life cycle environmental performance of products and organisations. In *OJ L* (No. 32021H2279; Vol. 471). European Commission. http://data.europa.eu/eli/reco/2021/2279/oj

European Commission. Joint Research Centre. (2018). *Development of a weighting approach for the environmental footprint.* Publications Office. https://doi.org/10.2760/945290

Eurostat. (2022). *Generation of waste by waste category, hazardousness and NACE Rev. 2 activity* [Dataset]. Eurostat. https://doi.org/10.2908/ENV%5C_WASGEN

Falk, S., Kluge Corrêa, N., Luccioni, S., Biber-Freudenberger, L., & Van Wynsberghe, A. (2026). From computation to environmental cost the resource burden of artificial intelligence. *Communications Earth & Environment*, *7*(1), 397. https://doi.org/10.1038/s43247-026-03537-5

Fantke, P., Jolliet, O., Evans, J. S., Apte, J. S., Cohen, A. J., Hänninen, O. O., Hurley, F., Jantunen, M. J., Jerrett, M., Levy, J. I., Loh, M. M., Marshall, J. D., Miller, B. G., Preiss, P., Spadaro, J. V., Tainio, M., Tuomisto, J. T., Weschler, C. J., & McKone, T. E. (2015). Health effects of fine particulate matter in life cycle impact assessment: Findings from the Basel Guidance Workshop. *The International Journal of Life Cycle Assessment*, *20*(2), 276–288. https://doi.org/10.1007/s11367-014-0822-2

Fraj, A. B., & Idir, R. (2017). Concrete based on recycled aggregates – Recycling and environmental analysis: A case study of paris' region. *Construction and Building Materials*, *157*, 952–964. https://doi.org/10.1016/j.conbuildmat.2017.09.059

Göbbels, L., Raulf, K., Orbatu, S., & Greiff, K. (2026). Advancing Real-Time Sensor-Based Quality Monitoring in Construction and Demolition Waste Processing for the Prediction of Weight-Based Particle Size Distributions. *Recycling*, *11*(6), 101. https://doi.org/10.3390/recycling11060101

GreenDelta GmbH. (2026). *openLCA* (Version 2.6) [Computer software]. https://www.openlca.org/

Guo, Z. (2023). Research on the Augmented Dickey-Fuller Test for Predicting Stock Prices and Returns. *Advances in Economics, Management and Political Sciences*, *44*(1), 101–106. https://doi.org/10.54254/2754-1169/44/20232198

International Organization for Standardization. (2006). *ISO 14040:2006 Environmental management—Life cycle assessment—Principles and framework*. International Organization for Standardization.

JAI A–S. (2025). *Specifications for SW-8000T-10GE* [Data sheet]. https://www.jai.com/products/sw-8000t-10ge/

Kabirifar, K., Mojtahedi, M., Wang, C., & Tam, V. W. Y. (2020). Construction and demolition waste management contributing factors coupled with reduce, reuse, and recycle strategies for effective waste management: A review. *Journal of Cleaner Production*, *263*, 121265. https://doi.org/10.1016/j.jclepro.2020.121265

Kirchherr, J., Piscicelli, L., Bour, R., Kostense-Smit, E., Muller, J., Huibrechtse-Truijens, A., & Hekkert, M. (2018). Barriers to the Circular Economy: Evidence From the European Union (EU). *Ecological Economics*, *150*, 264–272. https://doi.org/10.1016/j.ecolecon.2018.04.028

Kirchherr, J., Reike, D., & Hekkert, M. (2017). Conceptualizing the circular economy: An analysis of 114 definitions. *Resources, Conservation and Recycling*, *127*, 221–232. https://doi.org/10.1016/j.resconrec.2017.09.005

KLEEMANN GmbH. (2022). *Technische Informationen: MOBIREX MR 110(i) EVO2* [Data sheet]. KLEEMANN GmbH. https://www.kleemann.info/binary/full/o5256v101_Datasheet_kleemann_mr110evo2_de.pdf

König, M., Bosman, A. W., Hoos, H. H., & Rijn, J. N. van. (2024). Critically Assessing the State of the Art in Neural Network Verification. *Journal of Machine Learning Research*, *25*(12), 1–53.

Kranert, M. (Ed.). (2024). *Einführung in die Kreislaufwirtschaft: Planung, Recht, Verfahren* (6. Auflage). Springer Vieweg. https://doi.org/10.1007/978-3-658-41711-6

Kroell, N., Chen, X., Greiff, K., & Feil, A. (2022). Optical sensors and machine learning algorithms in sensor-based material flow characterization for mechanical recycling processes: A systematic literature review. *Waste Management*, *149*, 259–290. https://doi.org/10.1016/j.wasman.2022.05.015

Kroell, N., Thor, E., Göbbels, L., Schönfelder, P., & Chen, X. (2025). Deep learning-based prediction of particle size distributions in construction and demolition waste recycling using convolutional neural networks on 3D laser triangulation data. *Construction and Building Materials*, *466*, 140214. https://doi.org/10.1016/j.conbuildmat.2025.140214

Kromoser, B., Gappmaier, P., Ahmed, I., & Reichenbach, S. (2025). *Circular Economy in Concrete Construction Through Modular Construction, Automated Design and Production of Structurally Optimised Reusable Concrete Building Components*. SSRN. https://doi.org/10.2139/ssrn.5088411

Kronenwett, F., Maier, G., Leiss, N., Gruna, R., Thome, V., & Längle, T. (2024). Sensor-based characterization of construction and demolition waste at high occupancy densities using synthetic training data and deep learning. *Waste Management & Research: The Journal for a Sustainable Circular Economy*, *42*(9), 788–796. https://doi.org/10.1177/0734242X241231410

Lachat, A., Mantalovas, K., Desbois, T., Yazoghli-Marzouk, O., Colas, A.-S., Di Mino, G., & Feraille, A. (2021). From Buildings' End of Life to Aggregate Recycling under a Circular Economic Perspective: A Comparative Life Cycle Assessment Case Study. *Sustainability*, *13*(17), 9625. https://doi.org/10.3390/su13179625

Li, J., Fang, H., Fan, L., Yang, J., Ji, T., & Chen, Q. (2022). RGB-D fusion models for construction and demolition waste detection. *Waste Management*, *139*, 96–104. https://doi.org/10.1016/j.wasman.2021.12.021

Lubongo, C., Bin Daej, M. A. A., & Alexandridis, P. (2024). Recent Developments in Technology for Sorting Plastic for Recycling: The Emergence of Artificial Intelligence and the Rise of the Robots. *Recycling*, *9*(4), 59. https://doi.org/10.3390/recycling9040059

Ludbrook, J., & Dudley, H. (1998). Why Permutation Tests Are Superior to t and F Tests in Biomedical Research. *The American Statistician*, *52*(2), 127. https://doi.org/10.2307/2685470

Majuntke Logistik & Umwelt. (2026). *PREISLISTE 2026 Werk Attenhofen*. https://www.majuntke-umwelt.de/img/pdf/preisliste-kiesgrube-attenhofen.pdf

Moustafa, Z., Asif, M., & Wuni, I. Y. (2025). Circular economy in the building sector: A systematic review of environmental, economic, and social dimensions. *Sustainable Futures*, *9*, 100690. https://doi.org/10.1016/j.sftr.2025.100690

Mu, X., Zhang, X., He, G., & Liew, K. M. (2026). Toward low-carbon 3D concrete printing through circular construction and waste valorization. *Journal of Building Engineering*, *119*, 115308. https://doi.org/10.1016/j.jobe.2026.115308

Müller, A. (2018). *Baustoffrecycling: Entstehung - Aufbereitung - Verwertung*. Springer Fachmedien Wiesbaden. https://doi.org/10.1007/978-3-658-22988-7

Müller, A., & Martins, I. (2022). *Recycling of Building Materials: Generation-Processing-Utilization*. Springer Fachmedien Wiesbaden. https://doi.org/10.1007/978-3-658-34609-6

Osei-Tutu, S., Ayarkwa, J., Osei-Asibey, D., Nani, G., & Afful, A. E. (2023). Barriers impeding circular economy (CE) uptake in the construction industry. *Smart and Sustainable Built Environment*, *12*(4), 892–918. https://doi.org/10.1108/SASBE-03-2022-0049

Padilla-Rivera, A., Do Carmo, B. B. T., Arcese, G., & Merveille, N. (2021). Social circular economy indicators: Selection through fuzzy delphi method. *Sustainable Production and Consumption*, *26*, 101–110. https://doi.org/10.1016/j.spc.2020.09.015

planistar Lichttechnik GmbH. (2026). *Datenblatt & Bedienungsanleitung* [Data sheet]. https://downloads.datasheets-planistar.de/fileadmin/downloads/Datasheets2023/balkenleuchten/linienleuchten/datasheet_140-Xled-3-BZ-46w.pdf

Ruismäki, W., Zu Castell-Rüdenhausen, M., Pohjalainen, E., & Wahlström, M. (2025). Stakeholder perspectives on digital product passports for construction products. *Cleaner Logistics and Supply Chain*, *17*, 100275. https://doi.org/10.1016/j.clscn.2025.100275

Sachverständigenrat für Umweltfragen (Ed.). (2026). *Zirkulär bauen: Bestand erhalten, Kreisläufe schließen*. Geschäftsstelle des Sachverständigenrates für Umweltfragen (SRU).

Soto-Paz, J., Arroyo, O., Torres-Guevara, L. E., Parra-Orobio, B. A., & Casallas-Ojeda, M. (2023). The circular economy in the construction and demolition waste management: A comparative analysis in emerging and developed countries. *Journal of Building Engineering*, *78*, 107724. https://doi.org/10.1016/j.jobe.2023.107724

Sterk, E. (2023). *Willingness to Pay for Recycled Aggregates in Concrete Among German Construction Clients*. SSRN. https://doi.org/10.2139/ssrn.4583988

Szegedy, C., Zaremba, W., Sutskever, I., Bruna, J., Erhan, D., Goodfellow, I., & Fergus, R. (2013). *Intriguing properties of neural networks* (Version 4). arXiv. https://doi.org/10.48550/ARXIV.1312.6199

Tefa, L., Bianco, I., Blengini, G. A., & Bassani, M. (2022). Integrated and comparative Structural-LCA analysis of unbound and cement-stabilized construction and demolition waste aggregate for subbase road pavement layers formation. *Journal of Cleaner Production*, *352*, 131599. https://doi.org/10.1016/j.jclepro.2022.131599

Tighnavard Balasbaneh, A., & Ramadan, B. S. (2026). Integrating three pillars of sustainability for evaluating the modular construction building. *Construction Innovation*, *26*(2), 328–352. https://doi.org/10.1108/CI-01-2024-0002

TÜV Nord. (2026a). *Seminarangebot Abfallwirtschaft*. https://www.tuev-nord.de/de/weiterbildung/themen/abfallwirtschaft

TÜV Nord. (2026b). Weiterbildung: Einführung Data Science. *Seminare*. https://www.tuev-nord.de/de/weiterbildung/seminare/weiterbildung-einfuehrung-data-science

Varli, C., Göbbels, L., Raulf, K., Mirbach, B., Häberle, S., Lutz, M., Höhn, J., & Dehnen, G. (with Technische Informationsbibliothek (TIB)). (2026). *Verbundprojekt KIMBA - KI-basierte Prozesssteuerung und automatisiertes Qualitätsmanagement im Recycling von Bau- und Abbruchabfällen durch sensorbasiertes Inline-Monitoring von Korngrößenverteilungen: Sachbericht zum Verwendungsnachweis in der Fördermaßnahme Digital GreenTech - Umwelttechnik trifft Digitalisierung*. Hannover : Technische Informationsbibliothek. https://doi.org/10.34657/30283

Verein Deutscher Zementwerke. (2022). *Verbundvorhaben: R-Beton, Ressourcenschonender Beton—Werkstoff der nächsten Generation; Teilvorhaben 5: RC-Gesteinskörnung—Anwendung im Zement, Ökobilanzierung der Zement- und Betonherstellung, Bewertung der Alkaliempfindlichkeit: Schlussbericht zum Forschungsvorhaben "R-Beton": Schlussbericht zu Nr. 3.2 BNBest-BMBF 98—Teil I und Teil II* (Nos. 13N13125, 01154175). TIB Katalog. https://edocs.tib.eu/files/e01fb19/1666243779.pdf

Wernet, G., Bauer, C., Steubing, B., Reinhard, J., Moreno-Ruiz, E., & Weidema, B. (2016). The ecoinvent database version 3 (part I): Overview and methodology. *The International Journal of Life Cycle Assessment*, *21*(9), 1218–1230. https://doi.org/10.1007/s11367-016-1087-8

Zhou, Y., Thielmann, P., Chamoli, A., Mirbach, B., Stricker, D., & Raphael Rambach, J. (2025). ParticleSAM: Small Particle Segmentation for Material Quality Monitoring in Recycling Processes. *Proceedings of the 33rd European Signal Processing Conference (EUSIPCO 2025)*, *33*. arXiv:2508.03490. https://doi.org/10.48550/arXiv.2508.03490

Appendices

Appendix 1: Unit process tables

Table A1. Unit process table of the mobile comminution (pre-sieve, crusher and sieve), without sensor, DE

Economic flows, in						
Amount	**Unit**	**Product**	**Activity**	**Area**	**Data source**	**Process**
1.39E+01	MJ	Diesel, burned in building machine	Market for diesel, burned in building machine	GLO	Lachat et al. (2021); Fraj & Idir (2017); KLEEMANN GmbH (2022)	Loading into crusher and 371 kWh for operation
1.00E+00	Mg	Inert waste, for final disposal	Market for inert waste, for final disposal	CH	This study	Avoided emissions
1.00E-01	Mg • km	Transport, freight, lorry > 32 Mg, EURO4	Market for transport, freight, lorry > 32 Mg, EURO4	RER	Lachat et al. (2021); Fraj & Idir (2017)	Internal transport
Economic flows, out						
Amount	**Unit**	**Product**	**Activity**	**Area**	**Data source**	**Process**
1.00E+00	Mg	RA, without sensor	-	DE	This study	Reference flow

Table A2. Unit process table of the mobile comminution (pre-sieve, crusher and sieve), with sensor, DE

Economic flows, in						
Amount	**Unit**	**Product**	**Activity**	**Area**	**Data source**	**Process**
1.39E+01	MJ	Diesel, burned in building machine	Market for diesel, burned in building machine	GLO	Lachat et al. (2021); Fraj & Idir (2017); KLEEMANN GmbH (2022)	Loading into crusher and 371 kWh for operation
1.04E-06	Unit	Computer, laptop	Market for computer, laptop	GLO	Ecoinvent	4 years lifetime
1.60E-04	kWh	Electricity, low voltage	Market for electricity, low voltage	DE	This study	19.23 Wh for the operation of computer and sensor
1.00E+00	Mg	Inert waste, for final disposal	Market for inert waste, for final disposal	CH	This study	Avoided emissions
1.00E-01	Mg • km	Transport, freight, lorry > 32 Mg, EURO4	Market for transport, freight, lorry > 32 Mg, EURO4	RER	Lachat et al. (2021); Fraj & Idir (2017)	Internal transport
Economic flows, out						
Amount	**Unit**	**Product**	**Activity**	**Area**	**Data source**	**Process**
1.00E+00	Mg	RA, without sensor	-	DE	This study	Reference flow

Appendix 2: Autocorrelation Functions

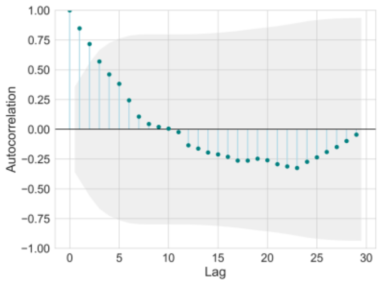

(a)

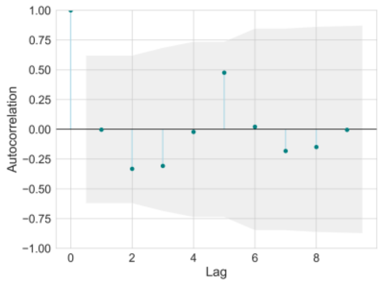

(b)

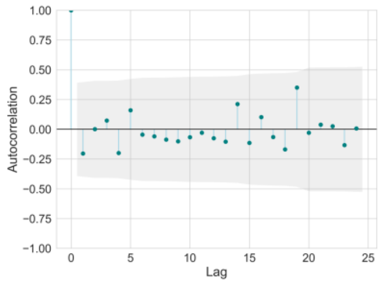

(c)

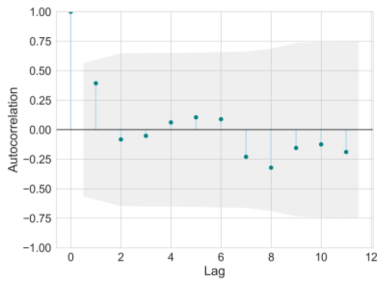

(d)

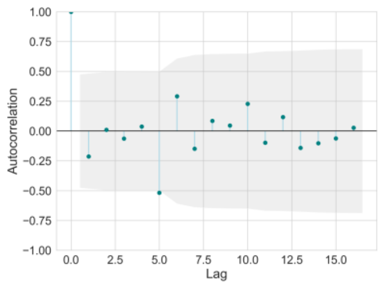

(e)

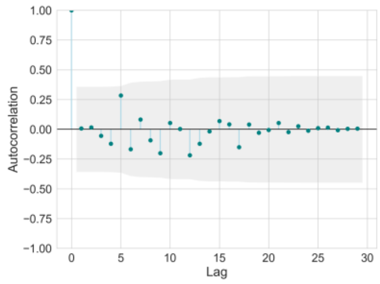

(f)

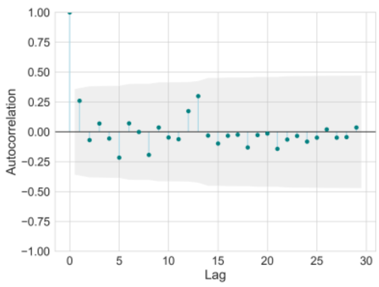

(g)

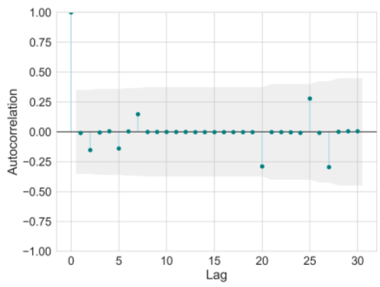

(h)

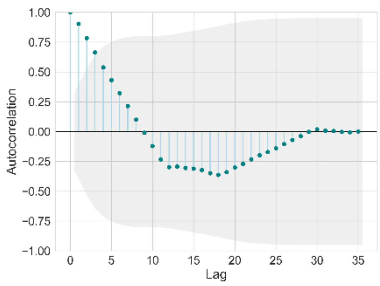

(i)

Figure A1. ACFs for each experiment. Figures (a)–(o) correspond to experiments A1–7, B1–7, and C in that particular order. The grey area in each plot refers to the significance bounds (i.e. outside the grey area means the autocorrelation is significant)

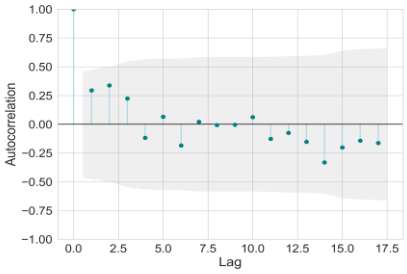

(j)

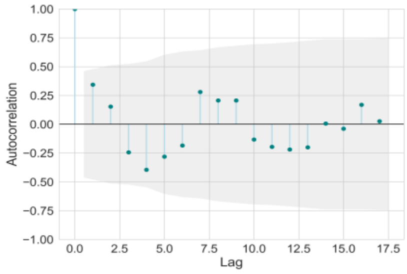

(k)

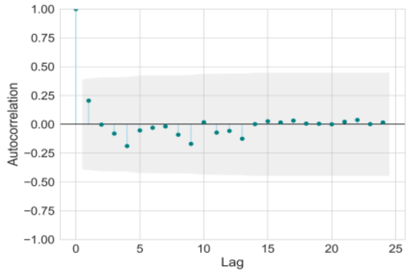

(l)

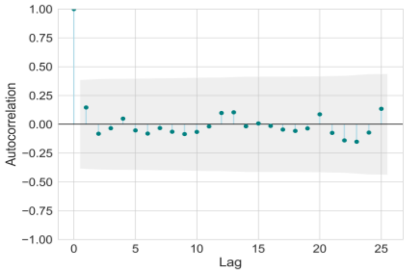

(m)

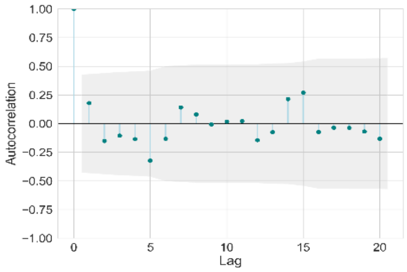

(n)

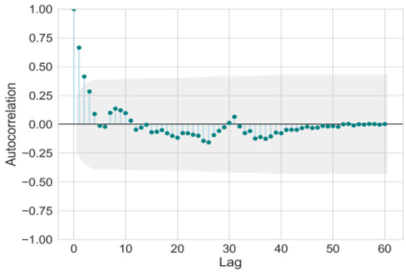

(o)

Figure A1 (Cont.). ACFs for each experiment. Figures (a)–(o) correspond to experiments A1–7, B1–7, and C in that particular order. The grey area in each plot refers to the significance bounds (i.e. outside the grey area means the autocorrelation is significant)

Appendix 3: Time Series

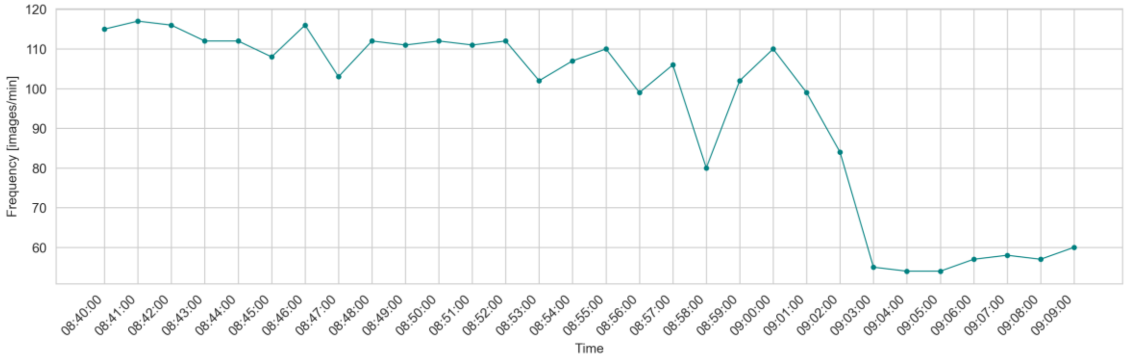

(**a**)

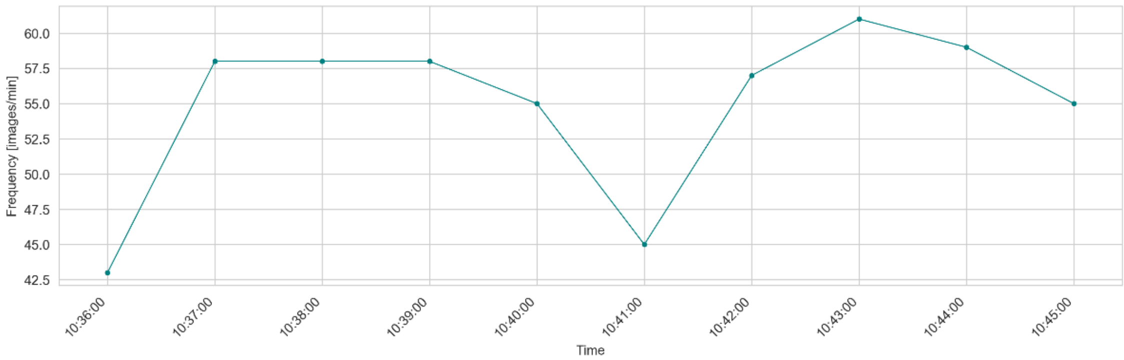

(**b**)

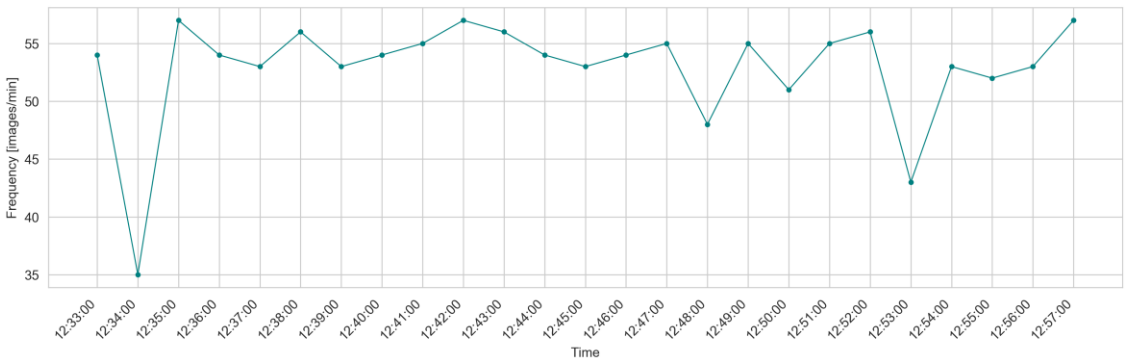

(**c**)

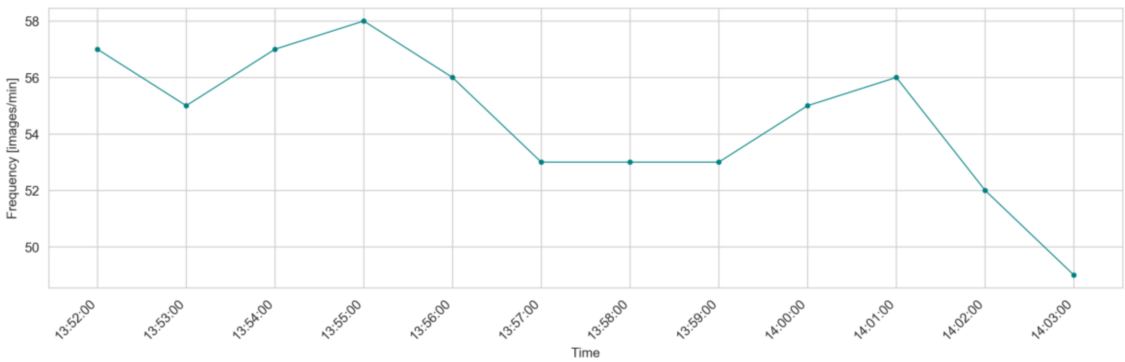

(**d**)

Figure A2. Time series plots for each experiment. Figures (a)–(o) correspond to experiments A1–7, B1–7, and C in that particular order

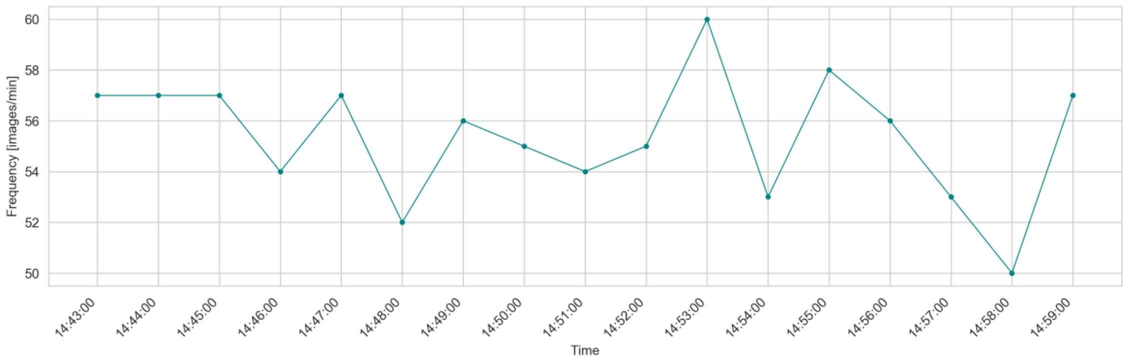

(e)

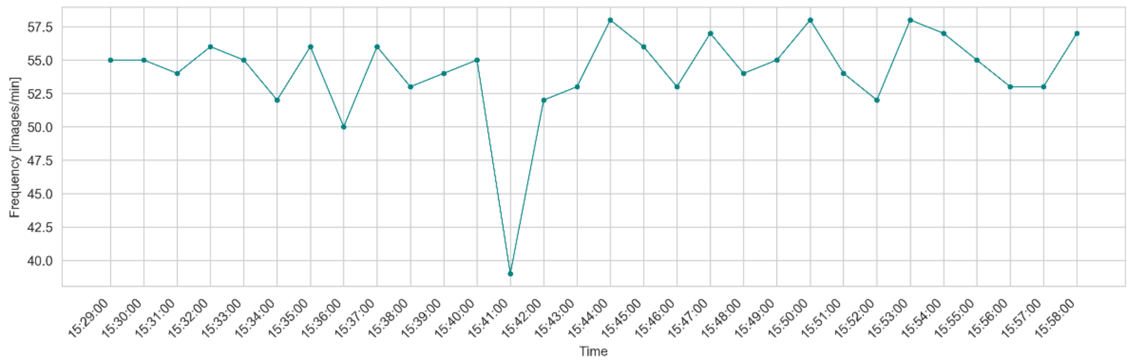

(f)

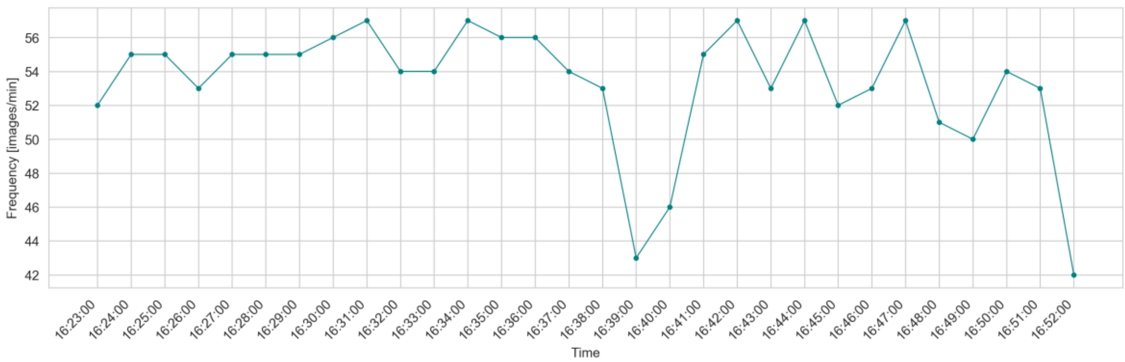

(g)

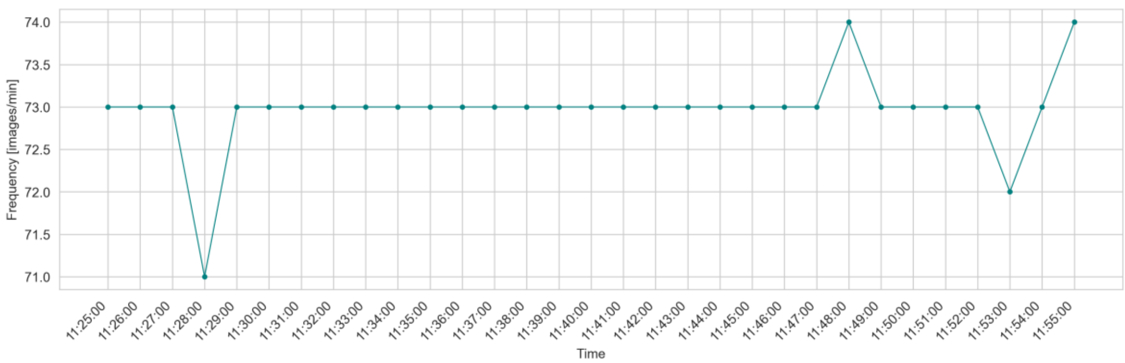

(h)

Figure A2 (Cont.). Time series plots for each experiment. Figures (a)–(o) correspond to experiments A1–7, B1–7, and C in that particular order.

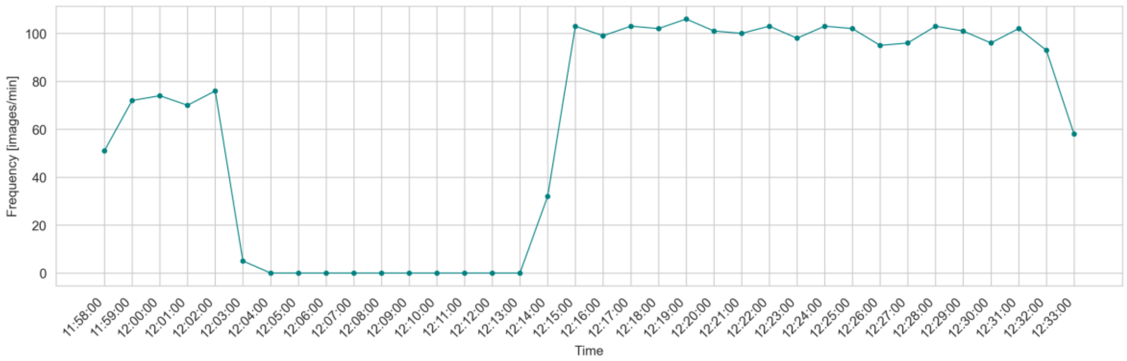

(i)

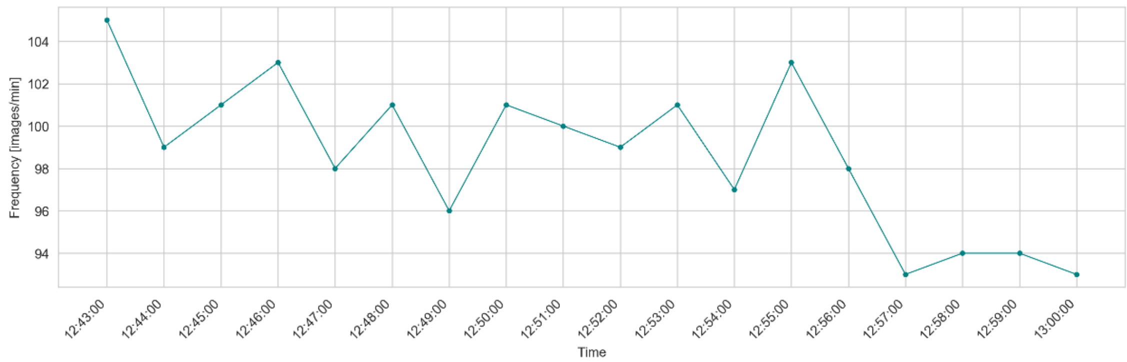

(j)

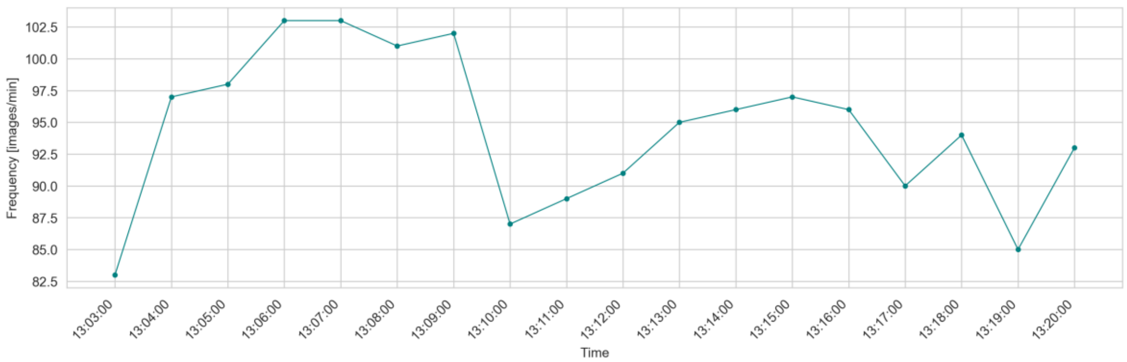

(k)

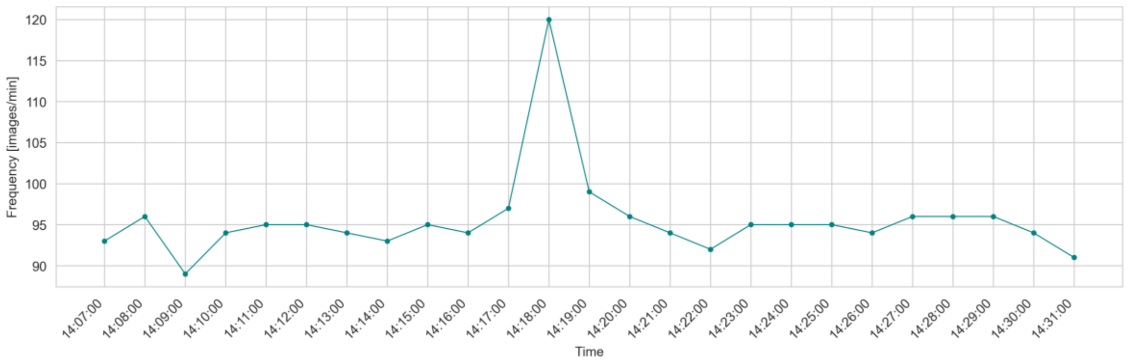

(l)

Figure A2 (Cont.). Time series plots for each experiment. Figures (a)–(o) correspond to experiments A1–7, B1–7, and C in that particular order.

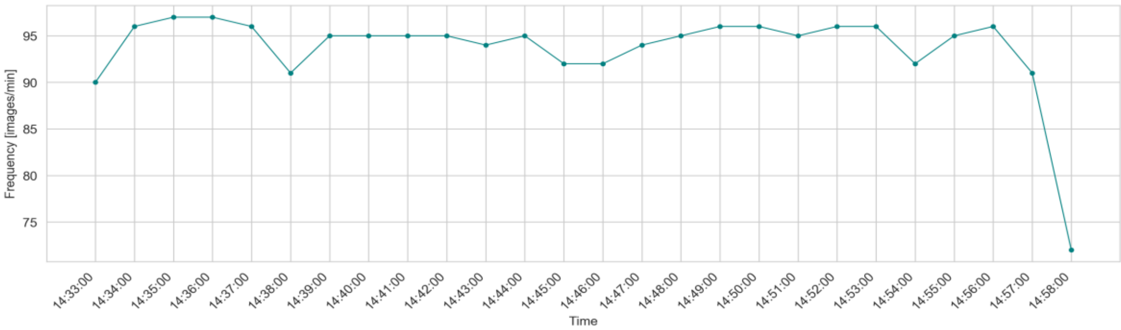

(m)

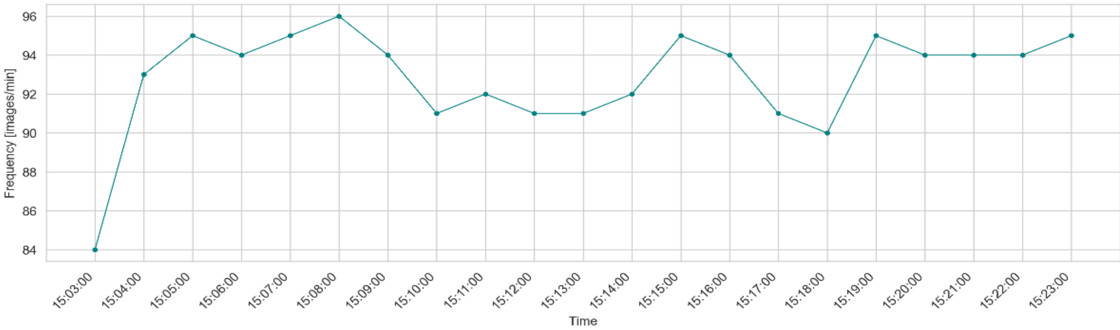

(n)

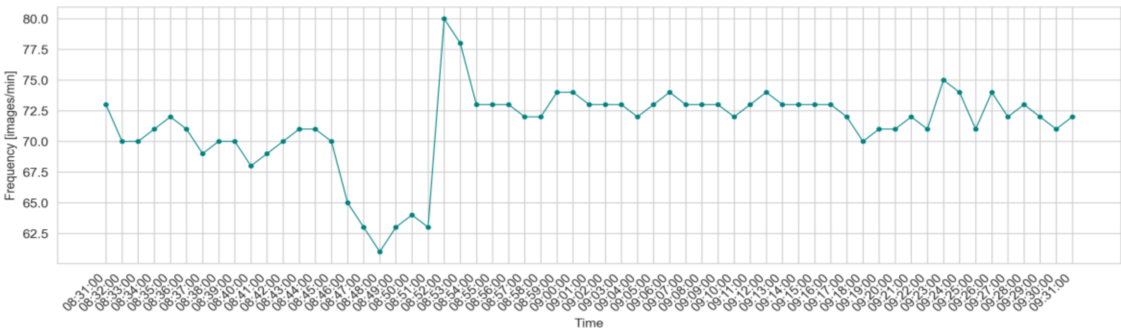

(o)

Figure A2 (Cont.). Time series plots for each experiment. Figures (a)–(o) correspond to experiments A1–7, B1–7, and C in that particular order.